JOURNAL OF GEOPHYSICAL RESEARCH, VOL. 103, NO. B7, PAGES 15,089–15,107, JULY 10, 1998

114.

# Shear wave splitting and upper mantle deformation in French Polynesia: Evidence for small-scale heterogeneity related to the Society hotspot

R. M. Russo[1]

Laboratoire de Tectonophysique, Université de Montpellier II, Montpellier, France

E. A. Okal

Department of Geological Sciences, Northwestern University, Evanston, Illinois

**Abstract.** We determined shear wave splitting parameters at four island sites in French Polynesia: Tiputa (TPT) on Rangiroa in the Tuamotu archipelago; Papeete (PPT) on Tahiti in the Society Islands; Tubuai (TBI) in the Cook-Austral island chain; and Rikitea (RKT) on Mangareva in the Gambier Islands. We also examined splitting at Pitcairn (PTCN) on Pitcairn Island; because of the short time of operation of PTCN, our results there are preliminary. We find substantial differences in splitting, most likely caused by variable upper mantle deformation beneath the five stations. At TPT the fast split shear wave ($\phi$) direction is N66°W±4°, parallel to the current Pacific-hotspots relative motion (APM) vector; the delay time between fast and slow waves is $1.3 \pm 0.2$ s. At PPT, on Tahiti, we could detect no splitting despite many clear *SKS* observations. At TBI, on Tubuai we detected splitting with a delay time of $1.1 \pm 0.1$ s and a $\phi$ direction midway between the local APM direction and the fossil spreading direction (N86°W±2° ), as locally indicated by the nearby Austral Fracture Zone. At RKT in the Gambier Islands, $\phi$ trends N53°W±6°, 16° clockwise of the local APM azimuth, and delay time at RKT is $1.1 \pm 0.1$ s. Results at PTCN include $\phi$ near N38°W±9° and a delay time of $1.1 \pm 0.3$ s. These different results imply variable upper mantle deformation beneath the five sites. We interpret splitting at TPT and, possibly, RKT as indicative of asthenospheric flow or shear in the APM direction beneath the stations. At PPT, azimuthal isotropy indicates deformed upper mantle with a vertical symmetry axis, or absence of strong or consistently oriented mantle deformation fabric beneath Tahiti. Either effect could be related to recent hotspot magmatism on Tahiti. At TBI, splitting may be complicated by juxtaposition of different lithospheric thicknesses along the nearby Austral Fracture Zone, resulting in perturbation of asthenospheric flow. The absence of splitting related to fossil spreading in French Polynesia indicates that upper mantle deformation processes postdating lithosphere formation are important at all four sites within that region. The $\phi$ azimuth at PTCN does not align with either the fossil direction or the APM direction, but our best individual determination of splitting parameters at this station lies within 10° of the local APM at Pitcairn Island.

## 1. Introduction

In the last decade, characterization of upper mantle deformation has become possible with the advent of shear-wave splitting measurements [*Bowman and Ando*, 1987; *Silver and Chan*, 1991; *Vinnik et al.*, 1989; *Helffrich et al.*, 1994; *Yang et al.*, 1995; *Gledhill and Gubbins*, 1996; *Russo et al.*, 1996]. Splitting of shear waves into two orthogonally polarized quasi-shear waves, one traveling slightly faster than the other, is primarily the result of systematic alignment of upper mantle minerals, most probably olivine, by plastic deformation as a consequence of flow in the upper mantle, an idea originally introduced by [*Hess* 1964]. To date, many splitting measurements utilizing the near-vertically incident phase *SKS* have been made for stable continental and

[1]Now at Department of Geological Sciences, Northwestern University, Evanston, Illinois.



Paper number 98JB01075.
0148-0227/98/98JB-01075$09.00

active tectonic regions. However, characterization of anisotropy in the ocean basins via shear wave splitting, despite a few studies [*Ansel and Nataf*, 1989; *Kuo and Forsyth*, 1992; *Su and Park*, 1994], has lagged behind that of continents because of the difficulties of ocean bottom seismometer deployment and because microseismic noise levels are much higher at island stations [*Wolfe and Silver*, 1998].

## 2. Tectonic Setting: French Polynesia and Pitcairn

The study region in the south-central Pacific, including the sites of the seismic stations (Tiputa, TPT; Papeete, PPT; Tubuai, TBI; Rikitea, RKT; and Pitcairn, PTCN), is shown in Figure 1. These stations lie on distinct bathymetric features: TPT is on Rangiroa atoll at the northwestern end of the Tuamotu Plateau [*Talandier and Okal*, 1987; *Ito et al.*, 1995]; PPT is on Tahiti in the Society Islands [*Duncan and McDougall*, 1976; *Okal and Batiza*, 1987]; and TBI is on Tubuai in the Cook-Austral Island chain [*Turner and Jarrard*, 1982]. The RKT site is on Mangareva in the Gambier Islands, and PTCN is on Pitcairn Island, both in the Gambier island chain. The three island stations PPT, TBI, and TPT lie between the Marquesas (north) and Austral (south) Fracture Zones, which juxtapose Pacific lithosphere of very different plate ages (Figure 1). Thus the lithosphere beneath these three stations apparently formed along the same spreading ridge segment, albeit at different times. The age of the original Pacific lithosphere beneath the stations differs by about 15 m.y. between TPT, on what should be the youngest Pacific lithosphere at around 72 m.y., and TBI, whose surrounding lithosphere formed about 88 m.y. ago [*Mueller et al.*, 1993]. The local age offset across the Marquesas Fracture Zone, in contrast, is around 25 m.y., and is 20 m.y. across the Austral Fracture Zone; in both cases plate age increases to the south of the fracture zone. RKT and PTCN lie SE of the Austral Fracture Zone in lithosphere that is 30 and 23 m.y. old, respectively [*Dupuy et al.*, 1993; *Mueller et al.*, 1993]. Both islands lie in the Pitcairn Island chain, which stretches from the active submarine Pitcairn hotspot [*Duncan et al.*, 1974;

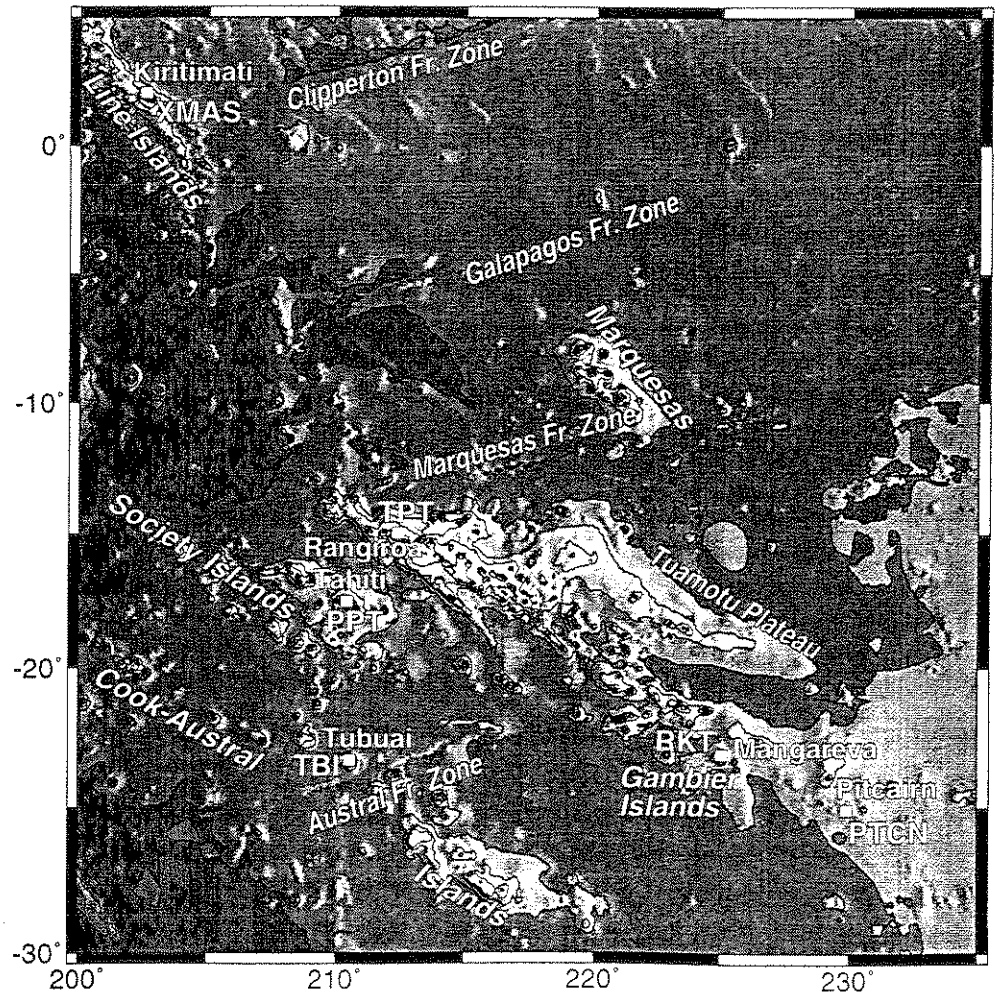


**Figure 1.** Map of French Polynesia study region. Seismic stations used in study shown as open squares. Bathymetry is ETOP05.

*Guillou et al.*, 1994], actually located some 80 km SE of Pitcairn island [*Stoffers et al.*, 1990] to Hereheretue atoll.

Although all the linear bathymetric features these island stations lie on are volcanic in origin [*Becker et al.*, 1974; *Dalrymple et al.*, 1975; *Duncan and McDougall*, 1976; *Schlanger et al.*, 1984; *Talandier and Okal*, 1987; *Woodhead and McCulloch*, 1989; *Dupuy et al.*, 1993; *Guillou et al.*, 1994; *Ito et al.*, 1995], with WNW-ESE linear trends approximately parallel to expected Pacific absolute (i.e., assumed fixed hotspots) plate motion, and hotspot origins have been proposed for all five [*Morgan*, 1972; *Duncan et al.*, 1974; *Jarrard and Clague*, 1977; *Okal and Cazenave*, 1985; *Okal and Batiza*, 1987; *Ito et al.*, 1995], significant differences in ages, history, and structure exist between the five islands. We outline the tectonic settings of the five sites, therefore, as a preface to our discussion of the results, below.

TPT, on Rangiroa, lies at the northwestern end of the southern Tuamotu island chain; the Tuamotu Plateau includes both northern and southern groups of islands in two approximately parallel chains (Figure 1). A few volcanic rocks aged 42 and 47 m.y. [*Schlanger et al.*, 1984] were dredged from the northwesternmost end of the Plateau, which is capped by thick limestone units [*Talandier and Okal*, 1987]. The northern Tuamotu chain terminates abruptly at the Marquesas Fracture Zone, perhaps indicative of a relation between the chain's formation and the Fracture Zone. The origin of the Plateau is unclear, but perhaps involves the activity of two (or even three) hotspots and a propagating ridge system; whether the hotspots were centered on the Pacific-Farallon ridge between 70 and 30 m.y. ago [*Okal and Cazenave*, 1985; *Talandier and Okal*, 1987], or whether the Plateau formed between 50 and 30 Ma, at around 600 km from this ridge on lithosphere 10-20 m.y. old [*Ito et al.*, 1995], is contested. The timing of the formation of individual islands on the plateau structure is also unknown.

PPT, on Tahiti, lies in the windward Society Islands (Figure 1). Unlike the Tuamotus, Tahiti has been the site of late Cenozoic hotspot volcanism: time of caldera collapse on the island is estimated at 1 Ma, and the last volcanism occurred only 400 thousand years ago [*Becker et al.*, 1974]. The current location of the Society hotspot lies 70-130 km east of Tahiti [*Talandier and Kuster*, 1976; *Cheminée et al.*, 1989]. Volcanic seismicity indicates that the Society Island chain has two active branches with an en échelon pattern of volcanism [*Talandier and Okal*, 1984].

TBI, on Tubuai, in the Cook-Austral Island chain (Figure 1) lies near the eastern end of the northern branch of the chain [*Turner and Jarrard*, 1982]. Formation of the Cook-Austral chain is difficult to reconcile with simple hotspot models, however. Both segments of the chain are marked by significant gaps in volcanism, and known age dates clearly violate the expected age progression along chain associated with normal hotspot tracks [*Okal and Batiza*, 1987]. Tubuai, for example, was volcanically active between 25 and 9 Ma [*Mottay*, 1976; *Turner and Jarrard*, 1982], and one rock suite on the island has been dated at 1 Ma, so it is possible that this island's volcanic history encompasses 24 m.y., an unexpectedly long duration for melts arising from a single oceanic hotspot. Ages of other islands in this chain lying NW of Tubuai (and which should thus be older, assuming a single, stationary hotspot and a northwestward moving Pacific plate) are also around 1 Ma (e.g., Rarotonga) and there is even evidence of an inverse age progression. The Cook-Austral chain is also the site of extreme variations in isotopic composition [*Hart*, 1984; *Okal and Batiza*, 1987] that perhaps signal great differences either in mantle reservoirs tapped by the associated hotspot(s), tremendous variability in the interaction of hotspot melts and Pacific lithosphere, or both.

RKT, on Mangareva in the Gambier Islands, lies in the central portion of the Pitcairn island chain. The Gambiers have been linked to Hereheretue atoll, the Duke of Gloucester islands, Mururoa and Fangataufa atolls, and Pitcairn Island to form a 1,900 km long island chain presumably formed by the Pitcairn hotspot [*Duncan et al.*, 1974; *Guillou et al.*, 1994]. Alkaline and tholeiitic volcanics occur on the several islands forming the Gambiers, each of which are remnants formed during caldera collapse from a single, much larger, volcanic island that predated them. K-Ar ages of volcanism range from 5.7 to 6.2 Ma [*Guillou et al.*, 1994]. The dated volcanism in the Gambiers is probably related to post hotspot subaerial activity, but the time of formation of the precursor island seems to be consistent with shield building during passage over the Pitcairn hotspot.

PTCN, on Pitcairn Island, lies some 80 km WNW of the current location of the Pitcairn hotspot [*Stoffers et al.*, 1990]. The hotspot itself is expressed as a series of seamounts formed of fresh volcanic edifices rising several thousand meters above surrounding seafloor; recent volcanic flows and extensive pillow lavas attest to the eruptive origin of the seamounts [*Binard et al.*, 1992]. Methane anomalies indicate the presence of active hydrothermal systems at the seamounts, but there is no indication of intervening volcanic activity between Pitcairn Island and the hotspot seamounts. *Dupuy et al.* [1993] suggest that isotopically distinct magmas present in the Gambiers and Pitcairn may be related to the degree of lithospheric melt which contributed to the sampled volcanic units; they claim Pitcairn shows increasing degree of lithospheric melting, which they infer from isotopic compositions of magmas from the post-erosional phase on that island. This is germane to our discussion because it seems to indicate that melting of the lithosphere is probable beneath Pitcairn during passage over the hotspot, and we are interested in processes that maintain or alter mantle fabrics.

## 3. Possible Sources of Splitting in French Polynesia

Given the significant variability in tectonic history and setting amongst the five sites, we briefly discuss potential sources of shear wave splitting in data recorded at these islands. Potential contributions to splitting from crustal minerals and crack alignment, as determined from observations of purely crustal $S$ wave paths, are limited to delay times (difference between fast and slow wave arrival times) of 0.1-0.3 s with a few extreme values near 0.5 s [*Silver and Chan*, 1991; *Silver*, 1996]. Yet the global average of splitting delay times from shear waves that traverse the upper mantle is just over 1 s [*Silver*, 1996], indicating that the upper mantle contribution to splitting is dominant. Three basic processes potentially result in significant upper mantle olivine fabric development in the study region: formation of upper mantle lithosphere at spreading ridges, and accretion of lithosphere from asthenosphere as the plate ages (which we refer to as "fossil spreading anisotropy"); flow in a more mobile and easily deformed asthenosphere below the lithosphere; and the perturbing effects of magma rise on both lithosphere and asthenosphere in the local regions of active hotspots. Combinations of all three processes could also affect the upper mantle regions beneath all the seismometer sites. Thus shear waves rising from the core-mantle boundary might become split traversing an anisotropic asthenosphere, and be split again in a differently anisotropic foliated and/or lineated upper mantle lithosphere. Nor can one rule out complications like channelized asthenospheric flow along the bases of fracture zones [*Vogt and Johnson*, 1975; *Epp*, 1984], or along any other relief on the lithosphere-asthenosphere boundary that might channel flow [*Sleep*, 1994; *Bormann et al.*, 1996].

The expected effects of these processes on upper mantle fabric, and thus on expected splitting parameters, can be readily estimated if we assume that the primary anisotropy-imparting mineral is olivine and that the upper mantle can therefore be closely approximated by a hexagonally symmetric medium resulting from development of linear preferred orientation (LPO) of olivine [*Hess*, 1964; *Silver and Chan*, 1991; *Mainprice and Silver*, 1993]. Oceanic lithosphere begins forming at spreading ridges and rapidly acquires a fabric from flow and freezing processes. Seismic refraction data [*Morris et al.*, 1969; *Francis*, 1969; *Shearer and Orcutt*, 1986], regional surface wave dispersion and tomographic studies [*Forsyth*, 1975; *Montagner and Nataf*, 1986; *Cara and Lévêque*, 1988; *Nishimura and Forsyth*, 1988, 1989; *Montagner and Tanimoto*, 1990, 1991], and analyses based on reflectivity and travel time anomalies [*Gaherty and Jordan*, 1996] confirm the significance of azimuthal anisotropy in the upper mantle and its relation to the deformation induced in olivine by mantle flow during the formation of oceanic lithosphere at ridges and during its subsequent thickening [*Carter et al.*, 1972; *Guéguen and Nicolas*, 1980; *Nicolas*, 1986; *Nicolas and Christensen*, 1987; *Ribe*, 1989; *Ribe and Yu*, 1991; *Tommasi et al.*, 1996]. These frozen flow fabrics preserve local flow directions and at large scale in the shallow lithosphere the resulting seismic anisotropy parallels the fossil spreading direction, delineated, for example, by fracture zones associated with the ridge that formed the lithosphere.

Beneath the ocean lithosphere, a clear seismic low-velocity zone interpreted as asthenospheric upper mantle [*Gutenberg*, 1926] is observable via dispersion of long-period surface waves [e.g., *Tanimoto and Anderson*, 1985], and through high-resolution surface wave overtone studies of the ocean basins [e.g., *Cara and Lévêque*, 1988]. This asthenospheric layer is the decoupling zone between oceanic plates and their underlying mesospheres, and therefore its deformation and hence its effect on splitting probably arises from shear caused by differential motion between plate and mesosphere. The Pacific plate, in particular, can be thought to be decoupled at the asthenosphere from a comparatively sluggish underlying mesosphere, given the analysis of *Forsyth and Uyeda* [1975] excluding basal drag forces as significant agents of the plate's dynamics. Thus flow in the asthenosphere would tend to align olivine crystals parallel to the direction of the Pacific plate's motion relative to the hotspots (APM), and we would expect to see shear waves traversing this asthenosphere split with their fast waves polarized in this direction [*Vinnik et al.*, 1989]. The delay time between fast and slow split waves in such a medium would depend mostly on the thickness of the deformed asthenospheric layer [*Tommasi et al.*, 1996].

Given that our data come from Pacific island sites, an important possible complication to upper mantle deformation here is the likelihood that hotspot volcanism and the establishment of hotspot conduits seriously affect the state of the mantle. The most likely effects of hotspots are reheating and thinning of the lithosphere [*Detrick and Crough*, 1978] and/or ponding of melts at the base of the lithosphere [*Sleep*, 1994], in either case leading to a reorientation of lithospheric olivine from the frozen fossil direction to new directions reflecting either propagation of hotspot melts through the lithosphere or the APM direction at time of hotspot activity. The latter process would presumably occur because weakening of the lithosphere, an effective volume increase of the asthenosphere, locally, would concentrate lithosphere-mesosphere relative motions preferentially within the weakest most plastic regions.

From the above considerations, three basic outcomes from searches for splitting parameters at Pacific island stations are possible: fast polarization directions may be parallel to fossil spreading directions, in which case the major contribution to the splitting signal is the unreconstituted lithosphere, virtually pristine as formed at the ridges. Or, fast polarization directions could be parallel to the local APM direction, in which case

the asthenospheric decoupling layer would be the primary source of splitting; or, over time, lithospheric olivine is somehow reoriented to the APM direction, perhaps by strain-induced recrystallization of either rotation or migration type [*Avé Lallemant and Carter*, 1970; *Guillope and Poirier*, 1979]. Finally, splitting could be more complex, perhaps reflecting complicated lithospheric anisotropy due to a long history of changing plate motions; presence of anisotropic lithosphere and asthenosphere, each characterized by a unique deformation; thermal erosion or deformation during magma ascent associated with hotspot plumes; flow along fracture zones or lithosphere-asthenosphere boundary topography; or some combination of all these effects.

## 4. Data

The data in our study were recorded on broadband seismometers at four stations of the Polynesian Seismic Network (Figure 1) and at Pitcairn. The instruments have an approximately flat magnification response between 1 and 100 s, and thus are ideal for recording shear waves with peak energy in the 5-20 s period range of most of our *SKS* and *S* data. The digital seismogram recording system used to archive the data includes filtration with a strong narrowband reject centered at 6 s to reduce microseismal noise related to sea swell. This filtration did not apparently affect our measurements adversely.

Details of the earthquakes we used are given in Table 1. For *SKS*, we limited ourselves to earthquakes farther than 88° epicentral angle so as to avoid contamination by *S* and *ScS* in the crossover distances of these phases. For *S* data, we used events at distances between 30° and 80° that were deeper than 410 km to avoid possible contamination by splitting at the source [e.g., *Kaneshima and Silver*, 1992; *Vinnik and Kind*, 1993; *Russo and Silver*, 1994]. We used the IASP91 [*Kennett and Engdahl*, 1991] Earth model as an aid in phase identification (see Figure 2), and we checked high signal-to-noise ratio seismograms of *SKS* particle motion in the horizontal plane for off-azimuth arrival and particle motion in the sagittal (i.e., vertical-radial) plane for unexpected incidence angles at the Earth's surface that could signal phase misidentifications or local structural heterogeneities that might corrupt results. In all cases, phases arrived on-azimuth within a tolerance of several degrees and at incidence angles of 10°-15° from vertical as expected for *SKS*. We examined all available data for events of magnitude $m_b \geq 5.7$ during the time period 1990 to mid-1995 fitting these criteria; for stations RKT and PTCN, we examined all such data during the operative life of the station to date. We also examined several events recorded earlier (1987-1990) during the installation of the broadband network, but this search was not exhaustive. In all, we examined seismograms for 66 events at PPT, 18 events at PTCN, 15 events at RKT, 38 events at TBI, and 22 events at TPT. From these we obtained 9 usable measurements at PPT, 4 at PTCN, 8 at RKT, 16 at TBI, and 6 at TPT (Table 1). A large majority of the seismograms we did not use were rejected because of low signal-to-noise. A few were unusable because of instrument problems such as obviously corrupted signal on one of the horizontal components. The majority of the data was usable, and we attempted to measure splitting on these seismograms, but the results often did not pass all four of our diagnostic criteria for good measurements (see below).

## 5. Methods

To analyze splitting of the shear wave phases we examined, we used two methods: the method of *Silver and Chan* [1991] and a more recently formulated method by *Wolfe and Silver* [1998]. Both methods rely on the assumption that the shear wave rising to the surface beneath the station from the core-mantle boundary is radially polarized. Energy on the transverse component of these shear waves is diagnostic of shear wave splitting caused by propagation through foliated and lineated olivine aggregates in the upper mantle beneath the recording station. The Silver and Chan method utilizes a grid search for the combination of splitting parameters $\phi$, the polarization direction of the fast split shear wave (azimuth from north), and $\delta t$, the delay time between fast and slow waves, that best minimizes energy on the transverse component of the seismogram, when used to reconstruct the rising shear wave prior to interaction with anisotropic layers. Both methods are also applicable for determination of splitting of *S* waves from deep ($h > 410$ km) earthquakes. In this case, the initial polarization of the phase is estimated from the data and splitting parameters derived from a minimization of energy on the component of motion corresponding to the smaller eigenvalue of the polarization matrix. A measurement is considered good if (1) there is clear energy on the transverse component (*SKS*) and the signal-to-noise ratio is better than about 5:1 (*S*, *SKS*); (2) the signal on the linearized transverse (*SKS*) or on the component corresponding to the minimum eigenvalue of the covariance matrix (*S*) is, after linearization, not distinguishable from noise outside the measurement window; (3) particle motion in the horizontal plane is elliptical before energy minimization, and is linear after energy minimization; (4) the contoured energy for the complete parameter space of the $\phi - \delta t$ grid search has a single well-defined minimum.

We also used the method of determining splitting parameters specifically developed by *Wolfe and Silver* [1998] for analysis of seismograms collected at ocean island stations: we search for the splitting parameters, $\phi$ and $\delta t$ that best fit, simultaneously, all the observed waveforms from a suite of *SKS* and/or *S* arrivals at the station. The method is based on the procedure of *Silver and Chan* [1991], and as they did, we calculated the smaller eigenvalue of the covariance matrix

**Table 1.** Single-Event Splitting Parameters

| Station | Date | Julian Day | Time, UT | Latitude, deg | Longitude, deg | Depth, km | Magnitude | Baz,[a] deg | Phase | $\phi$, deg | $\delta t$, s | Result |
|---|---|---|---|---|---|---|---|---|---|---|---|---|
| PPT | May 12, 1990 | 132 | 0450:08.7 | 48.940 | 141.380 | 606.0 | 6.5 | 322 | *SKS* | -38 ±22 | — — | null |
| PPT | May 2, 1993 | 122 | 1126:54.8 | -56.415 | -24.491 | 13.0 | 6.3 | 152 | *SKS* | -37 ±22 | — — | null |
| PPT | Aug. 7, 1993 | 219 | 0000:37.0 | 26.585 | 125.610 | 155.0 | 6.0 | 297 | *SKS* | -74 ±22 | — — | null |
| PPT | May 10, 1994 | 130 | 0636:28.3 | -28.501 | -63.096 | 601.0 | 6.4 | 116 | *S* | -52 ±22 | — — | null |
| PPT | July 21, 1994 | 202 | 1836:31.7 | 42.340 | 132.870 | 471.0 | 6.5 | 313 | *SKS* | -46 ±22 | — — | null |
| PPT | Sept. 28, 1994 | 271 | 1639:51.6 | -5.786 | 110.350 | 638.0 | 5.9 | 261 | *SKS* | 81 ±22 | — — | null |
| PPT | Nov. 4, 1994 | 308 | 0113:20.1 | -9.397 | -71.334 | 591.0 | 5.8 | 96 | *S* | -76 ±22 | — — | null |
| PPT | Jan. 6, 1995 | 006 | 2237:37.9 | 40.246 | 142.180 | 27.0 | 6.7 | 315 | *SKS* | -45 ±12 | — — | null |
| PPT | April 21, 1995 | 111 | 0009:56.2 | 11.999 | 125.700 | 33.0 | 6.1 | 283 | *SKS* | -77 ±20 | — — | null |
| PTCN | March 21, 1997 | 080 | 1207:17.6 | -31.163 | 179.624 | 449.0 | 5.6 | 250 | *S* | -83 ±9 | 2.8 ±.6 | |
| PTCN | March 25, 1997 | 084 | 1644:32.6 | -9.063 | -71.295 | 603.0 | 5.4 | 85 | *S* | 73 ±22 | — — | null |
| PTCN | March 26, 1997 | 085 | 0208:57.2 | 51.277 | 179.533 | 33.0 | 6.0 | 331 | *SKS* | -29 ±22 | — — | null |
| PTCN | April 23, 1997 | 113 | 1944:28.4 | 13.986 | 144.901 | 101.0 | 6.2 | 285 | *SKS* | -75 ±22 | — — | null |
| RKT | Dec. 25, 1995 | 359 | 0443:24.5 | -6.903 | 129.151 | 141.0 | 6.3 | 261 | *SKS* | -62 ±13 | 1.1 ±.3 | |
| RKT | Jan. 1, 1996 | 001 | 0805:10.8 | 0.729 | 119.931 | 24.0 | 6.3 | 265 | *SKS* | -63 ±14 | 1.2 ±.3 | |
| RKT | Feb. 7, 1996 | 038 | 2136:46.3 | 45.324 | 149.892 | 42.0 | 6.3 | 317 | *SKS* | -43 ±22 | — — | null |
| RKT | May 2, 1996 | 123 | 1334:29.0 | -4.548 | 154.833 | 500.0 | 5.6 | 274 | *S* | -62 ±9 | 2.2 ±.4 | poor |
| RKT | June 21, 1996 | 173 | 1357:10.0 | 51.568 | 159.119 | 20.0 | 6.0 | 325 | *SKS* | -35 ±22 | — — | null |
| RKT | July 22, 1996 | 204 | 1419:35.7 | 1.340 | 120.650 | 28.0 | 7.0 | 265 | *SKS* | -43 ±9 | 1.7 ±.3 | poor |
| RKT | Aug. 5, 1996 | 228 | 2238:22.0 | -20.720 | -178.160 | 555.0 | 7.4 | 265 | *S* | -79 ±11 | 1.7 ±.4 | poor |
| RKT | Oct. 18, 1996 | 292 | 1050:20.8 | 30.470 | 131.290 | 22.0 | 6.6 | 297 | *SKS* | -63 ±22 | — — | null |
| TBI | Dec. 10, 1993 | 344 | 0859:35.8 | 20.912 | 121.280 | 12.0 | 5.8 | 289 | *SKS* | -70 ±22 | — — | null |
| TBI | Jan. 10, 1994 | 010 | 1553:50.1 | -13.339 | -69.446 | 589.0 | 6.4 | 99 | *S* | -37 ±5 | 1.8 ±.6 | poor |
| TBI | April 29, 1994 | 119 | 0711:29.6 | -28.299 | -63.252 | 562.0 | 6.3 | 115 | *S* | 27 ±12 | 1.0 ±.4 | poor |
| TBI | May 3, 1994 | 123 | 1636:43.6 | 10.241 | -60.758 | 36.0 | 5.8 | 80 | *SKS* | -87 ±6 | 2.3 ±.4 | poor |
| TBI | May 10, 1994 | 130 | 0636:28.3 | -28.501 | -63.096 | 601.0 | 6.4 | 115 | *S* | 32 ±6 | 1.4 ±.7 | poor |
| TBI | May 23, 1994 | 143 | 0536:01.6 | 24.065 | 122.560 | 20.0 | 5.7 | 293 | *SKS* | -73 ±22 | — — | null |
| TBI | May 29, 1994 | 149 | 1411:50.9 | 20.556 | 94.160 | 36.0 | 6.2 | 281 | *SKS* | -79 ±22 | — — | null |
| TBI | May 29, 1994 | 149 | 1411:50.9 | 20.556 | 94.160 | 36.0 | 6.2 | 281 | *SKS* | -79 ±22 | — — | null |
| TBI | Aug. 19, 1994 | 231 | 1002:51.8 | -26.642 | -63.421 | 564.0 | 6.4 | 113 | *S* | 19 ±7 | 1.5 ±.7 | poor |
| TBI | Nov. 4, 1994 | 308 | 0113:20.1 | -9.379 | -71.334 | 591.0 | 5.8 | 94 | *S* | -80 ±8 | 2.1 ±.7 | poor |
| TBI | Nov. 14, 1994 | 318 | 1915:30.6 | 13.525 | 121.070 | 32.0 | 6.1 | 283 | *SKS* | -77 ±22 | — — | null |
| TBI | Nov. 15, 1994 | 319 | 2018:11.3 | -5.589 | 110.190 | 561.0 | 6.2 | 261 | *SKS* | 86 ±1 | 3.2 ±.5 | poor |
| TBI | Jan. 6, 1995 | 006 | 2237:37.9 | 40.246 | 142.180 | 27.0 | 6.7 | 315 | *SKS* | -69 ±5 | 1.9 ±.3 | |
| TBI | April 17, 1995 | 107 | 2328:08.3 | 45.904 | 151.290 | 34.0 | 6.1 | 323 | *SKS* | -49 ±3 | — — | poor |
| TBI | April 21, 1995 | 111 | 0009:56.2 | 11.999 | 125.700 | 33.0 | 6.1 | 283 | *SKS* | -77 ±22 | — — | null |
| TBI | May 5, 1995 | 125 | 0353:47.6 | 12.622 | 125.310 | 33.0 | 6.2 | 283 | *SKS* | -77 ±14 | — — | null |
| TBI | June 11, 1996 | 163 | 1822:55.7 | 12.610 | 125.150 | 33.0 | 6.0 | 283 | *SKS* | -77 ±2 | — — | null |
| TPT | May 12, 1990 | 132 | 0450:08.7 | 48.940 | 141.380 | 606.0 | 6.5 | 321 | *SKS* | -56 ±3 | 2.7 ±.4 | |
| TPT | May 2, 1993 | 122 | 1126:54.8 | -56.415 | -24.491 | 13.0 | 6.3 | 152 | *SKS* | -39 ±22 | — — | poor |
| TPT | Jan. 10, 1994 | 010 | 1553:50.1 | -13.339 | -69.446 | 589.0 | 6.4 | 100 | *S* | -21 ±22 | — — | null |
| TPT | April 29, 1994 | 119 | 0711:29.6 | -28.299 | -63.252 | 562.0 | 6.3 | 116 | *S* | -65 ±22 | — — | null |
| TPT | May 10, 1994 | 130 | 0636:28.3 | -28.501 | -63.096 | 601.0 | 6.4 | 117 | *S* | -60 ±22 | — — | null |
| TPT | May 24, 1994 | 144 | 0400:42.1 | 23.959 | 122.450 | 16.0 | 6.2 | 293 | *SKS* | -67 ±22 | — — | null |
| TPT | July 21, 1994 | 202 | 1836:31.7 | 42.340 | 132.870 | 471.0 | 6.5 | 313 | *SKS* | -46 ±22 | — — | null |
| XMAS | Sept. 4, 1997 | 247 | 0423:36.5 | -26.535 | 178.322 | 618.0 | 6.8 | 218 | *S* | -58 ±8 | 2.5 ±.2 | |

[a]Baz, backazimuth.

of corrected particle motion for each value of candidate polarization directions (0° to ±90°) and delay time (0 to 4 s). We then normalized the energy surface corresponding to each of the seismograms within the suite by its minimum value and summed the results to find the splitting parameters corresponding to the most linearized corrected particle motion for the whole suite of events. Errors were estimated in a fashion similar to

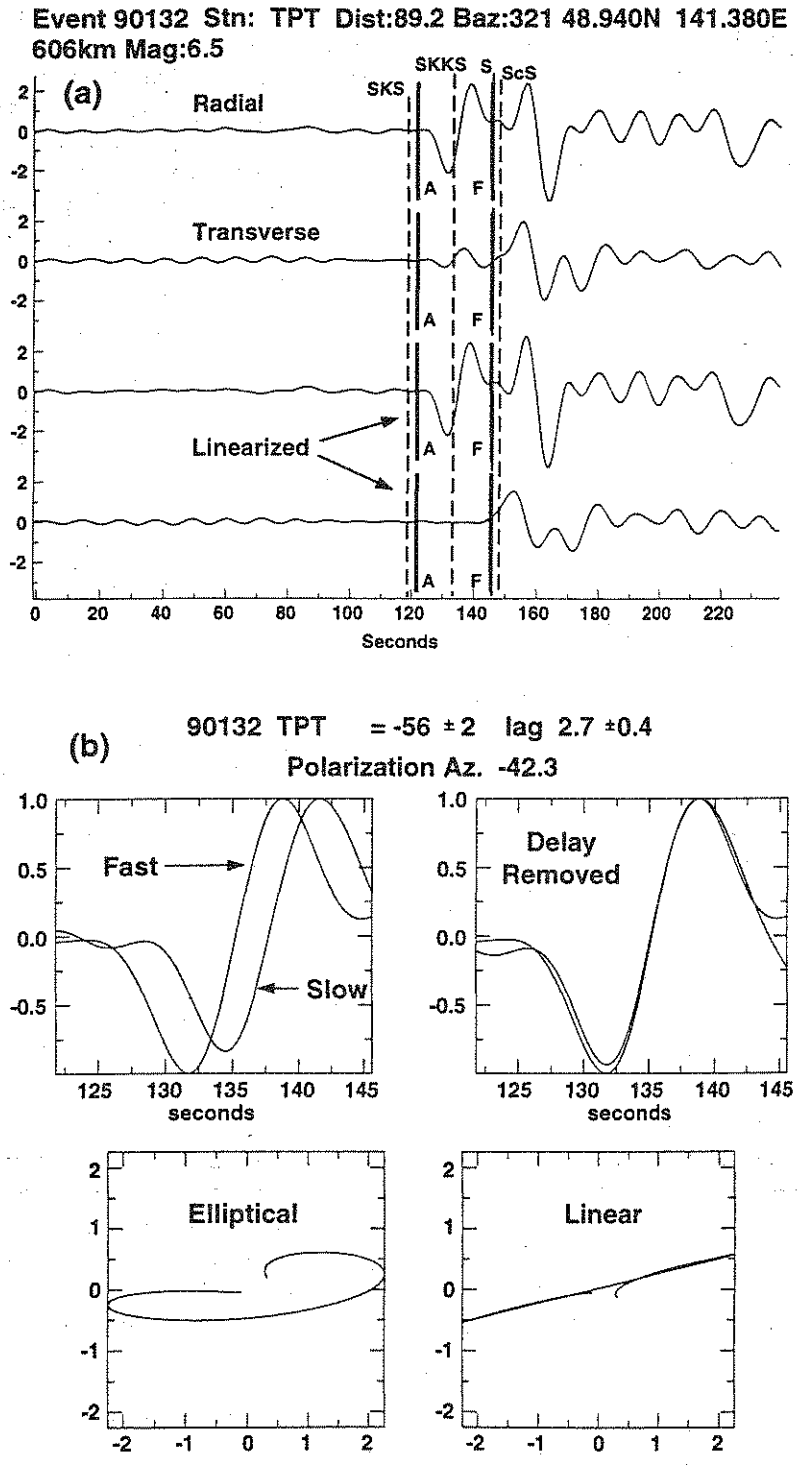


**Figure 2.** Example of individual splitting measurement at station TPT. Event is 1990 Julian day 132 (see Table 1). (a) Original waveforms (radial, transverse) before linearization are top two traces; bottom two traces are linearized waveforms. Measurement window marked by A and F. Expected arrival times of shear waves phases calculated from IASP91 Earth model shown as vertical dashed lines. Note *SKS* signal on transverse phase, but low signal to noise ratio. (b) Fast and slow waveforms from measurement window and particle motions. (top left) Fast and slow waveforms in the fast and slow reference frame. (top right) Same waveforms, delay removed; note excellent waveform coherence. (bottom left) Particle motion of waveforms in upper left frame; note clear ellipticity. (bottom right) Linearized particle motion of delay-removed phases. (c) Contours of energy on transverse component for the full range of candidate $\phi$ and $\delta t$. Minimum energy denoted by star. Note large uncertainty in delay time.

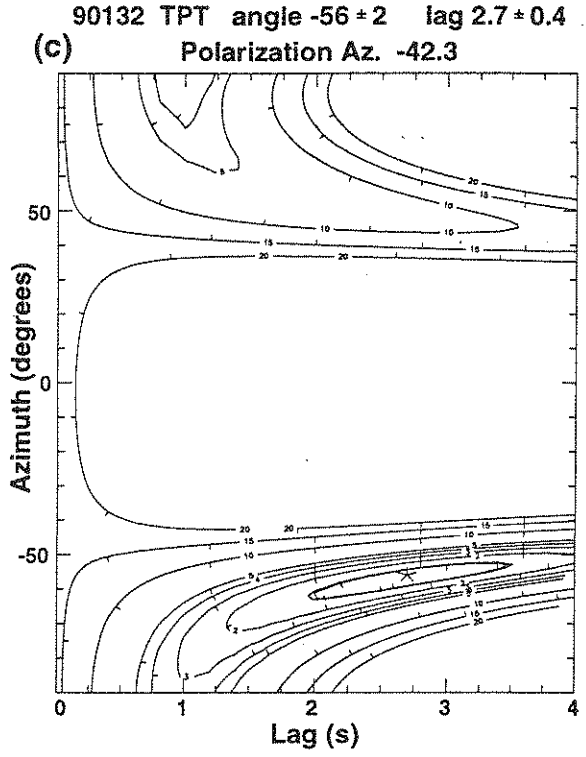


**Figure 2.** (continued)

that of *Silver and Chan* [1991] by assuming that the minimum value of the covariance matrix eigenvalue is a sum-of-squares noise process that is $\chi^2$ distributed, estimating the total number of degrees of freedom in the system by summing the calculated degrees of freedom for each transverse record after linearization and then determining a 95% confidence limit. We emphasize that this method does not involve stacking of data within the measurement windows, but rather only summing of the normalized energy surfaces corresponding to the complete azimuth-delay time grid search. The result is the best fitting splitting parameters for all the included data. These results are easier to interpret objectively since they yield a single set of splitting parameters with errors rather than a range of less well constrained parameters which may encompass a range of interpretive possibilities.

We used events from varying back azimuths whenever possible in order to evaluate better the assumption of horizontal symmetry axis, single-layer anisotropy inherent in the Silver and Chan method. This is effective because splitting parameters vary as functions of back azimuth if symmetry axes dip or more than one anisotropic layer is present [*Babuźska et al.*, 1993; *Silver and Savage*, 1994]. (We note that the scatter in splitting parameters we observe for the individual event measurements do not match the variations expected if two anisotropic layers are present.) Barring such complications, the method yields the best single-layer splitting parameters for the given suite of data.

The simultaneous linearization technique is particularly necessary for island station data because microseismic noise levels can be high and because of greater shear wave attenuation beneath the oceans. Typically, noise is great enough to degrade splitting measurements at island stations, and most recorded $S$ waves must be low-pass filtered at periods greater than 10 s to be detected. Thus individual measurements of splitting delay time (on the order of 1 s) and of fast polarization axis orientation may have large errors: for example, published values of splitting parameters at Hawaii (KIP) range in azimuth (clockwise from north) from 25° to 90° [*Vinnik et al.*, 1989; *Ansel and Nataf*, 1989; *Kuo and Forsyth*, 1992]. This value was constrained to 90° ± 5° by *Wolfe and Silver* [1998] using their multiple data technique.

## 6. Results: Splitting in French Polynesia and at Pitcairn

Use of the *Silver and Chan* [1991] splitting method for single *SKS* and $S$ phases yielded highly variable results (Table 1). In much of the data, energy on the transverse component the primary diagnostic of splitting of the core shear wave phases is apparent to the eye, but low signal-to-noise ratios degrade the measurements. Many of the seismograms that appear to include split shear waves result in "null" (i.e., no resolvable splitting parameters) or nearly null (almost no resolution of delay time) measurements. Nevertheless, at TPT, TBI, RKT, and PTCN we found some clear evidence of splitting, and we were able to make several moderately good measurements. For PPT, however, all the data we examined yielded no clear evidence of splitting.

Because the results from the individual measurements did not satisfactorily reflect the evidence of splitting we could see in the seismograms of at least four of the stations, and because of the significant scatter in the results of these individual measurements (see Table 1), we then applied the newer *Wolfe and Silver* [1998] method to the data. The events we used and the splitting parameters we determined via the simultaneous linearization method at the four Polynesian stations and at Pitcairn are detailed in Tables 2 and 3. For PPT, we stacked seven events (four $S$ and three *SKS* phases; Table 2) which yielded the results shown in Figure 3: we can exclude delay times over 0.1 s for all orientations of $\phi$ so the mantle beneath PPT is azimuthally isotropic within the limits of our ability to measure it for the available data. For TBI, on Tubuai in the Cook-Austral chain, $\phi$ is N86°W and the delay time is 1.1 s, as determined from a simultaneous linearization of four events recorded at that station. Splitting parameters for 5 events at TPT are $\phi$ of N66°W and 1.3 s delay (Figure 4). Four RKT events linearized simultaneously yielded a $\phi$ of N53°W and a delay time of 1.1 s. Four different events recorded at PTCN yield a simultaneously linearized $\phi$ of N38°W, and a delay time of 1.1 s. We

**Table 2.** Station Stack Event Information

| Date | Julian Day | Time, UT | Latitude, deg | Longitude, deg | Depth, km | Magnitude | Distance, deg | Baz,[a] deg | Phase | Station |
|---|---|---|---|---|---|---|---|---|---|---|
| Aug. 7, 1993 | 219 | 0000:37.0 | 26.585 | 125.610 | 155.0 | 6.0 | 93 | 297 | *SKS* | PPT |
| May 10, 1994 | 130 | 0636:28.3 | -28.501 | -63.096 | 601.0 | 6.4 | 79 | 116 | *S* | PPT |
| July 21, 1994 | 202 | 1836:31.7 | 42.340 | 132.870 | 471.0 | 6.5 | 93 | 313 | *SKS* | PPT |
| Sept. 28, 1994 | 271 | 1639:51.6 | -5.786 | 110.350 | 638.0 | 5.9 | 98 | 261 | *SKS* | PPT |
| Nov. 4, 1994 | 308 | 0113:20.1 | -9.397 | -71.334 | 591.0 | 5.8 | 76 | 96 | *S* | PPT |
| Jan. 6, 1995 | 006 | 2237:37.9 | 40.246 | 142.180 | 27.0 | 6.7 | 86 | 314 | *S* | PPT |
| May 5, 1995 | 125 | 0353:47.6 | 12.622 | 125.310 | 33.0 | 6.2 | 89 | 283 | *S* | PPT |
| March 21, 1997 | 080 | 1207:17.6 | -31.163 | 179.624 | 449.0 | 5.6 | 45 | 250 | *S* | PTCN |
| March 25, 1997 | 084 | 1644:32.6 | -9.063 | -71.295 | 603.0 | 5.4 | 58 | 85 | *S* | PTCN |
| March 26, 1997 | 085 | 0208:57.2 | 51.277 | 179.533 | 33.0 | 6.0 | 88 | 331 | *SKS* | PTCN |
| April 23, 1997 | 113 | 1944:28.4 | 13.986 | 144.901 | 101.0 | 6.2 | 92 | 285 | *SKS* | PTCN |
| Dec. 25, 1995 | 359 | 0443:24.5 | -6.903 | 129.151 | 141.0 | 6.3 | 93 | 261 | *SKS* | RKT |
| Jan. 1, 1996 | 001 | 0805:10.8 | 0.729 | 119.931 | 24.0 | 6.3 | 104 | 265 | *SKS* | RKT |
| July 22, 1996 | 204 | 1419:35.7 | 1.340 | 120.650 | 28.0 | 7.0 | 104 | 265 | *SKS* | RKT |
| Oct. 18, 1996 | 292 | 1050:20.8 | 30.470 | 131.290 | 22.0 | 6.6 | 105 | 297 | *SKS* | RKT |
| May 10, 1994 | 130 | 0636:28.3 | -28.501 | -63.096 | 601.0 | 6.4 | 76 | 115 | *S* | TBI |
| Aug. 19, 1994 | 231 | 1002:51.8 | -26.642 | -63.421 | 564.0 | 6.4 | 77 | 113 | *S* | TBI |
| Nov. 15, 1994 | 319 | 2018:11.3 | -5.589 | 110.190 | 561.0 | 6.2 | 97 | 261 | *SKS* | TBI |
| Jan. 6, 1995 | 006 | 2237:37.9 | 40.246 | 142.180 | 27.0 | 6.7 | 90 | 315 | *SKS* | TBI |
| May 12, 1990 | 132 | 0450:08.7 | 48.940 | 141.380 | 606.0 | 6.5 | 89 | 321 | *SKS* | TPT |
| May 2, 1993 | 122 | 1126:54.8 | -56.415 | -24.491 | 13.0 | 6.3 | 95 | 152 | *SKS* | TPT |
| April 29, 1994 | 119 | 0711:29.6 | -28.299 | -63.252 | 562.0 | 6.3 | 78 | 116 | *S* | TPT |
| May 10, 1994 | 130 | 0636:28.3 | -28.501 | -63.096 | 601.0 | 6.4 | 78 | 117 | *S* | TPT |
| July 21, 1994 | 202 | 1836:31.7 | 42.340 | 132.870 | 471.0 | 6.5 | 92 | 313 | *SKS* | TPT |

[a]Baz, backazimuth.

also estimated splitting parameters for more and different seismograms at the five stations, but the results did not vary significantly from those quoted.

## 7. Discussion

We first address the apparent failure of the individual measurements to constrain splitting parameters at the five stations. Two observations are germane: First, signal-to-noise ratios were low, even when *SKS* energy was apparent on the transverse components of seismograms (Figure 2a). Second, the result of this is visible even in the individual measurements we judged best (Figure 2b), which show that although the polarization of the fast wave is fairly well established (confidence ellipses are narrow with respect to azimuth), delay times are much more poorly resolved (the ellipses are very long in the delay time direction). We infer that this is because the noise interferes more strongly with the small-amplitude transverse energy, swamping it enough, in effect, to render delay time estimation difficult. Because such noise is inherently uncorrelated, whereas the splitting should be the same, for different events recorded at the stations, the stacking method allows a better estimation of the splitting delay time. For this reason, we have greater confidence in the quality of the simultaneous linearization measurements than in the individual measurements we made for the five sta-

**Table 3.** Station Locations and Stacked Splitting Parameters

| Code | Name | Site | South Latitude, deg | West Longitude, deg | $\phi$, deg | $\delta t$, s |
|---|---|---|---|---|---|---|
| PPT | Papeete | Tahiti | 17.569 | 149.432 | isotropic | |
| PTCN | Pitcairn | Pitcairn | 25.073 | 130.095 | -38 ±9 | 1.1 ±0.3 |
| RKT | Rikitea | Rikitea | 23.118 | 134.972 | -53 ±6 | 1.1 ±0.1 |
| TBI | Tubuai | Tubuai | 23.349 | 149.461 | -86 ±2 | 1.1 ±0.1 |
| TPT | Tiputa | Rangiroa | 14.984 | 147.619 | -66 ±4 | 1.3 ±0.2 |

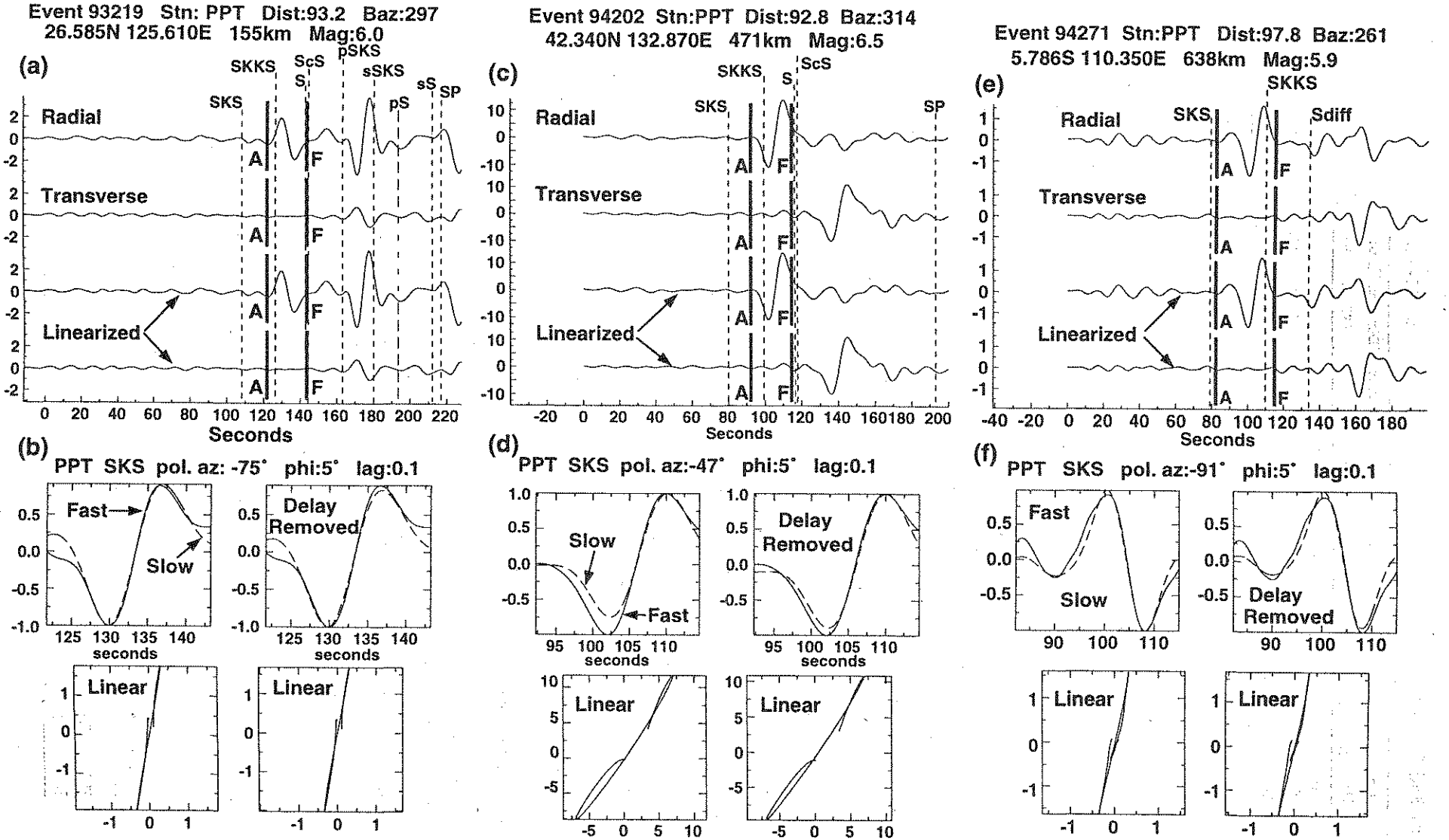


**Figure 3.** Example of waveforms and splitting determination at PPT for a stack of seven events (Table 2). (a) Waveforms for event 93219. Note no transverse *SKS* energy. (b) Event 93219 waveforms in fast-slow frame and corresponding particle motions. Note particle motion is always linear, sign of no splitting. (c) Waveforms for event 94202. (d) Event 94202 waveforms in the fast-slow frame and corresponding particle motions. (e) Waveforms for event 94271. (f) Event 94271 waveforms in the fast-slow frame and corresponding particle motions. (g) Contoured energy for the stack of seven PPT events. Note splitting delay times greater than 0.1 s are excluded at 95% confidence limit (contour marked 1).

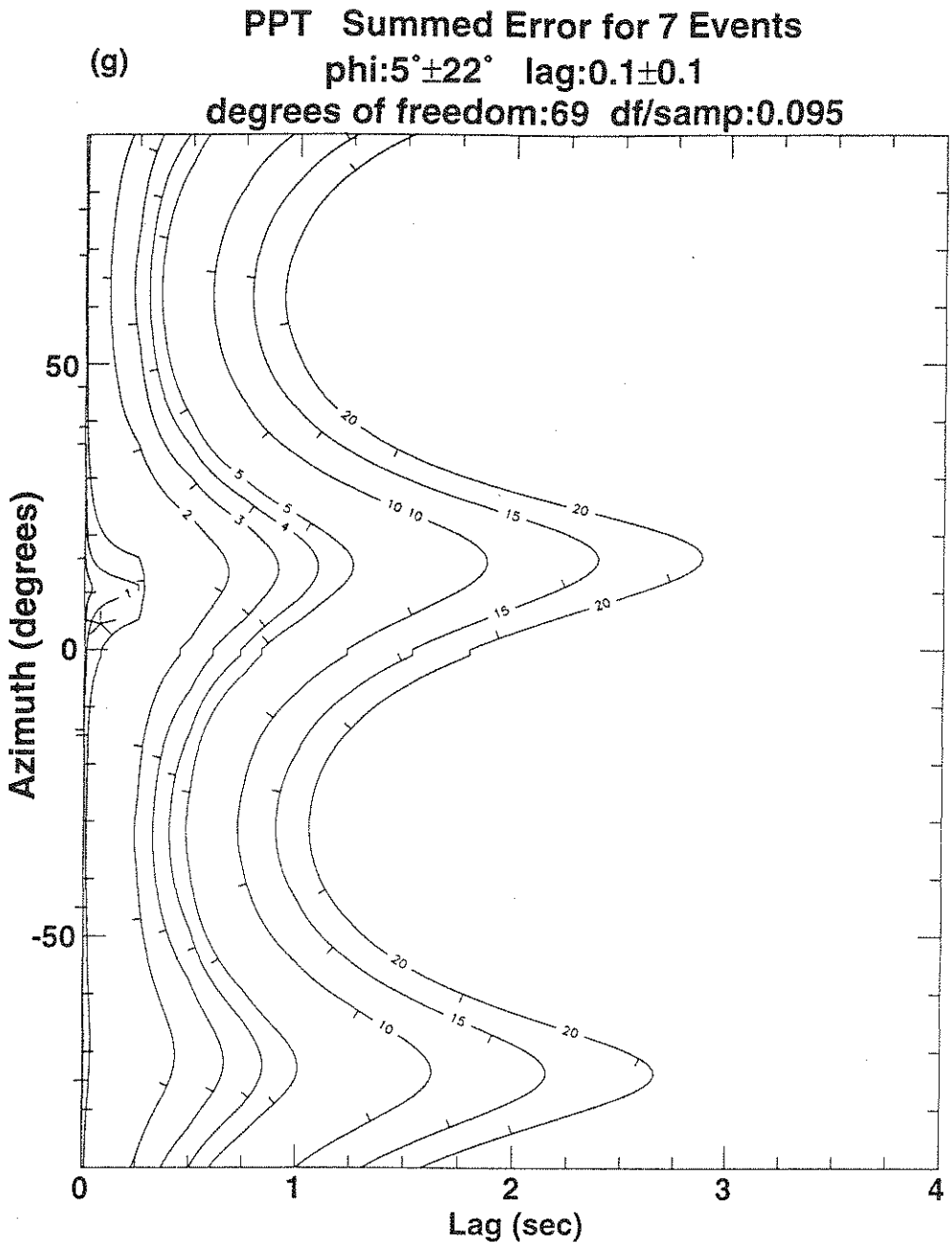


**Figure 3.** (continued)

tions, and we limit our interpretations to the results of the multiple event procedure (Figures 3, 4, and 5).

### 7.1. TPT, Tuamotu Plateau

The results at the five stations demonstrate that significant variation in splitting (and therefore in upper mantle deformation) occurs at relatively small scale in French Polynesia (Figure 6). Four stations, TPT in the NW Tuamotu Plateau, TBI in the Cook-Austral chain, and RKT and PTCN in the Pitcairn chain, clearly lie above significant thicknesses (100 to 150 km) of deformed upper mantle, but PPT, on Tahiti, apparently does not. Within the context of possible anisotropy-forming mechanisms we discussed above, the results at TPT could be explained two ways. The fast polarization direction at TPT, N66°W, is parallel to the Tuamotu chain underlying Rangiroa, and is also parallel to the Pacific plate's motion relative to Pacific hotspots. The splitting could be engendered in the asthenosphere beneath TPT, caused by shear in the upper mantle low-velocity zone between the base of Pacific lithosphere and deeper mesosphere. In contrast, this result cannot be related to fossil lithospheric fabrics, which should be parallel to nearby fracture zones (Figure 6). The splitting fast polarization direction we measured at TPT is consistent with the analysis of *Talandier and Bouchon* [1979], who showed that $P_n$ azimuthal anisotropy in the

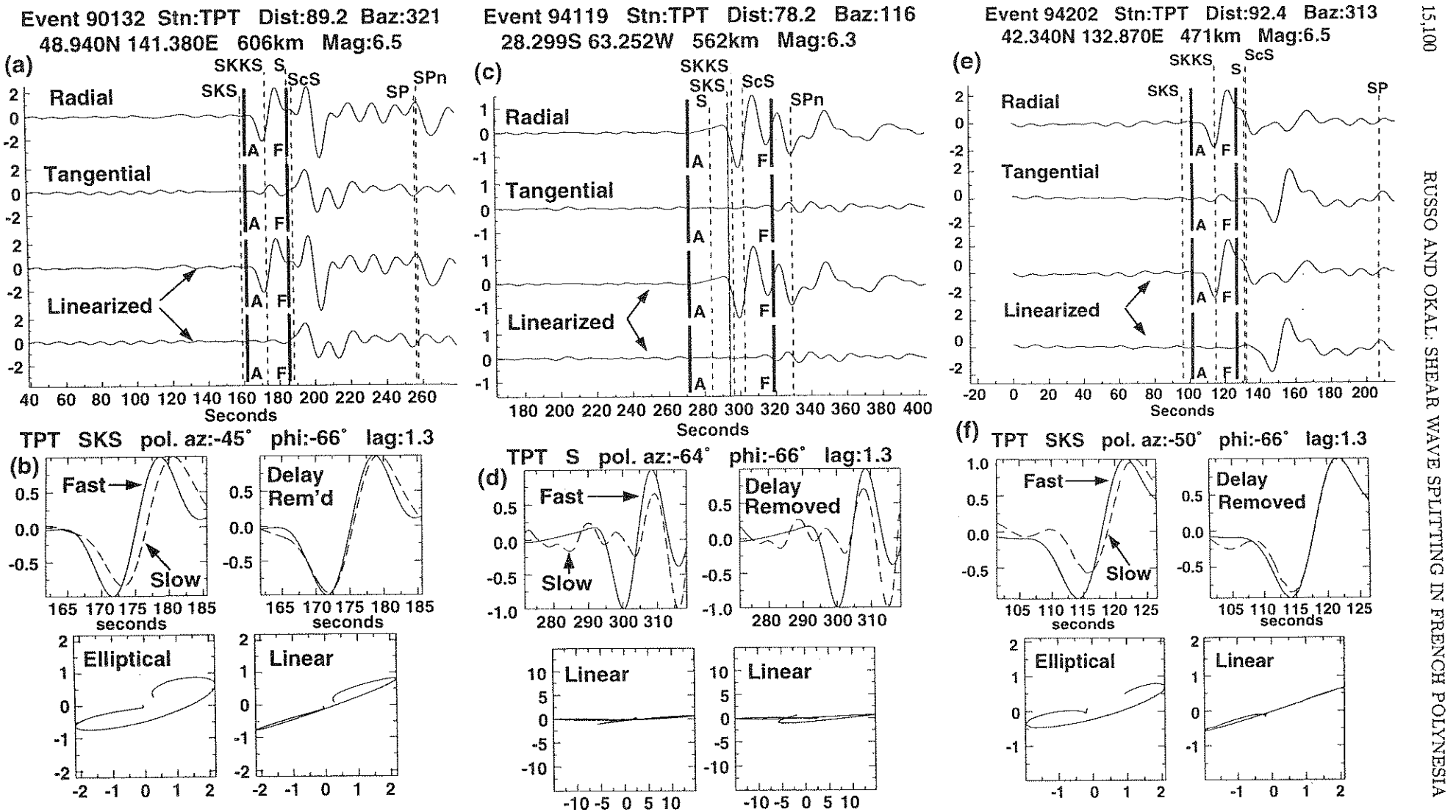


**Figure 4.** Example of waveforms and splitting determination at TPT for a stack of 5 events (Table 2). (a) Waveforms for event 90132. Note clear transverse *SKS* energy. (b) Event 90132 waveforms in fast-slow frame and corresponding particle motions. Note particle motion before delay removal is elliptical, sign of splitting. (c) Waveforms for event 94119. (d) Event 94119 waveforms in fast-slow frame and corresponding particle motions. (e) Waveforms for event 94202. (f) 94202 waveforms in the fast-slow frame and corresponding particle motions. (g) Contoured energy for the stack of five TPT events. Best splitting parameters (star, within double contour) are constrained to be $\phi N66°\mathrm{W}$, delay time $\sim 1.3$ s.

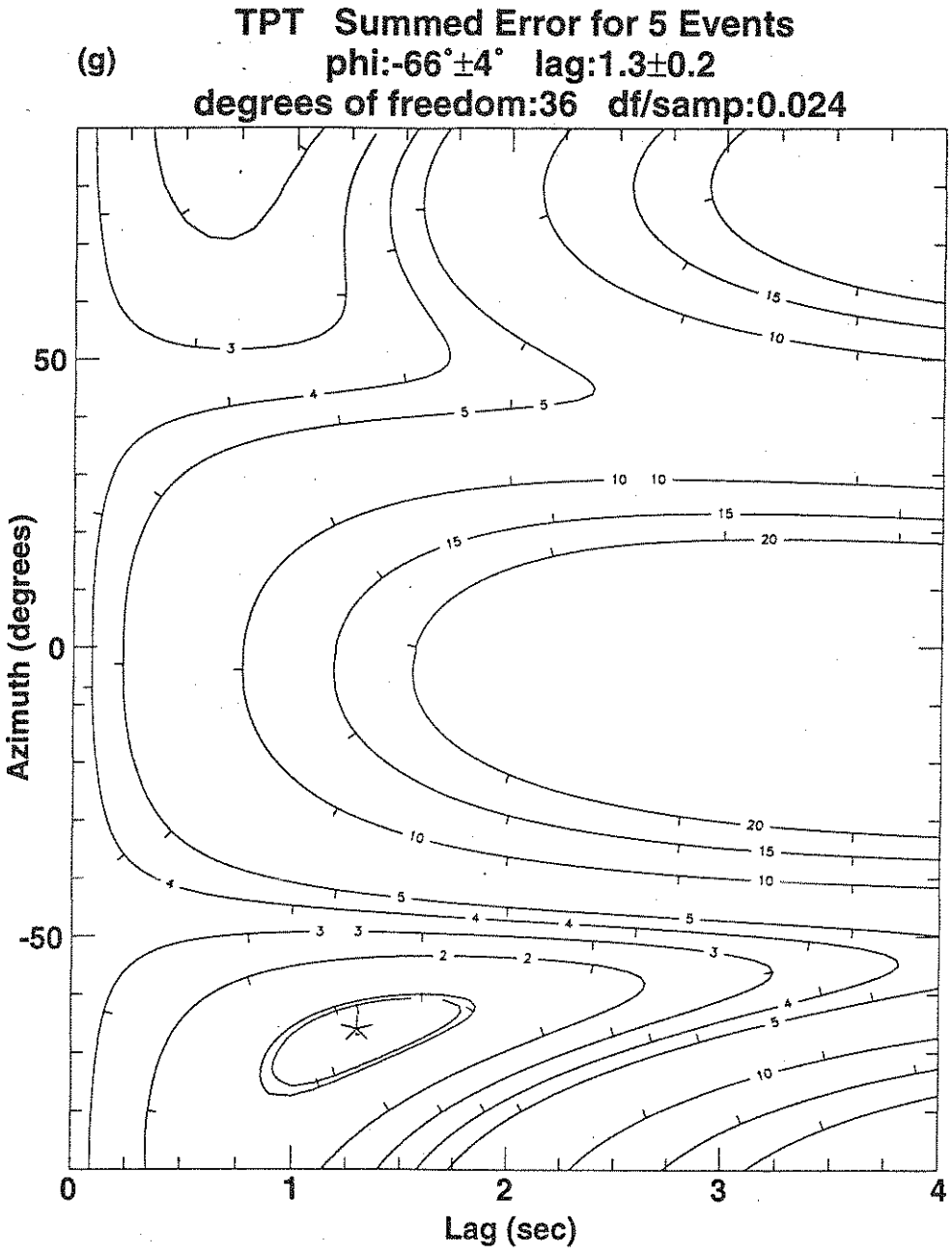


**Figure 4.** (continued)

Polynesian province is oriented fast-axis parallel to the island chains and local APM direction.

The possibility that the shear wave splitting at TPT arises only from the asthenosphere is interesting because on the basis of surface wave studies [*Forsyth*, 1975; *Nishimura and Forsyth*, 1988, 1989; *Montagner and Tanimoto*, 1990, 1991] and refraction experiments [*Hess*, 1964; *Francis*, 1969; *Morris et al.*, 1969; *Shearer and Orcutt*, 1986], we expect oceanic mantle lithosphere to have a fossil fabric and, given lithospheric age and corresponding thickness at TPT, that this lithosphere should contribute significantly to the splitting. Absence of clear evidence for a lithospheric contribution at TPT can be ascribed to the reheating effect of hotspots [*Detrick and Crough*, 1978; *Sleep*, 1994], which may destroy fossil lithospheric olivine fabrics through dynamic recrystallization. If this is so, it implies temperatures sufficiently high to call into question the definition of such upper mantle as lithospheric. The emplacement of the 30 km thick crust [*Talandier and Okal*, 1987] of the Tuamotu Plateau, by one or more hotspots and/or a propagating ridge segment [*Okal and Cazenave*, 1985; *Ito et al.*, 1995] may have altered sub-TPT lithospheric mantle fabrics formed previously at the Pacific-Farallon Ridge. If the post-Plateau emplacement lithospheric mantle fabrics were weakly developed (e.g., randomly oriented olivine crystals), then the lithosphere would not contribute to the observed splitting. The paral-

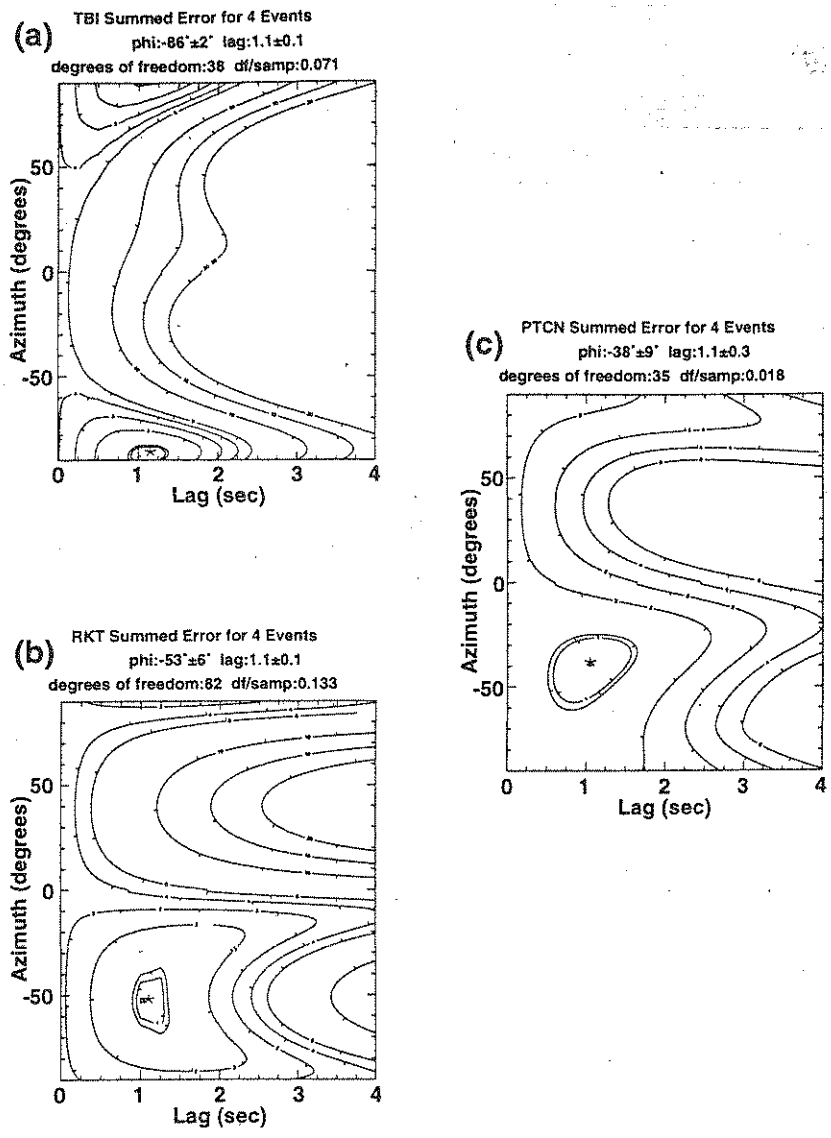


**Figure 5.** (a) Summed contours of energy corresponding to either the transverse component or smaller eigenvalue of the polarization matrix for four events at station TBI. Note grid search yields a single good estimate of splitting parameters that best linearize the four events simultaneously (star). (b) Same as Figure 5a, but for four events at station RKT. (c) Same as Figure 5a, but for four events at station PTCN.

lelism of the fast polarization direction at TPT and the Pacific-hotspots APM would thus arise solely from the sub-Tuamotu asthenosphere, and this fact would place no temporal constraint on the time of formation of the Plateau.

A variation on the idea of an asthenospheric source of the TPT splitting, consistent with the surface wave and $P_n$ data, is that hotspot reheating could have formed a horizontal channel of asthenosphere by thermal erosion cutting up into the base of an otherwise horizontal lithosphere-asthenosphere boundary [*Sleep*, 1994; *Bormann et al.*, 1996]. This thermal erosion might erase fossil lithospheric fabrics, replacing lithosphere by asthenosphere in a channel trending in the APM direction (post 43 Ma formation of the channel therefore required). A localized channel might not have a large effect on surface waves, and, if filled by asthenospheric mantle, could explain the observed shallow low $P_n$ and $S_n$ velocities.

The alternative to solely asthenospheric anisotropy in the sub-TPT upper mantle is that the source of anisotropy is lithospheric, but that the fossil spreading fabric in the sub-Tuamotu lithosphere has been destroyed and replaced by APM-parallel fabrics. Evidence in support of such an idea is the existence of the thick, linear, grossly APM-parallel Tuamotu Plateau, whose emplacement via hotspot volcanism probably had a strong effect on surrounding lithosphere. Again, the pervasive deformation required to reorient existent fabrics in the lithosphere calls into question, if only locally, the concept of a rigid, little-deforming plate. Heated and deformed (asthenospheric?) upper mantle would

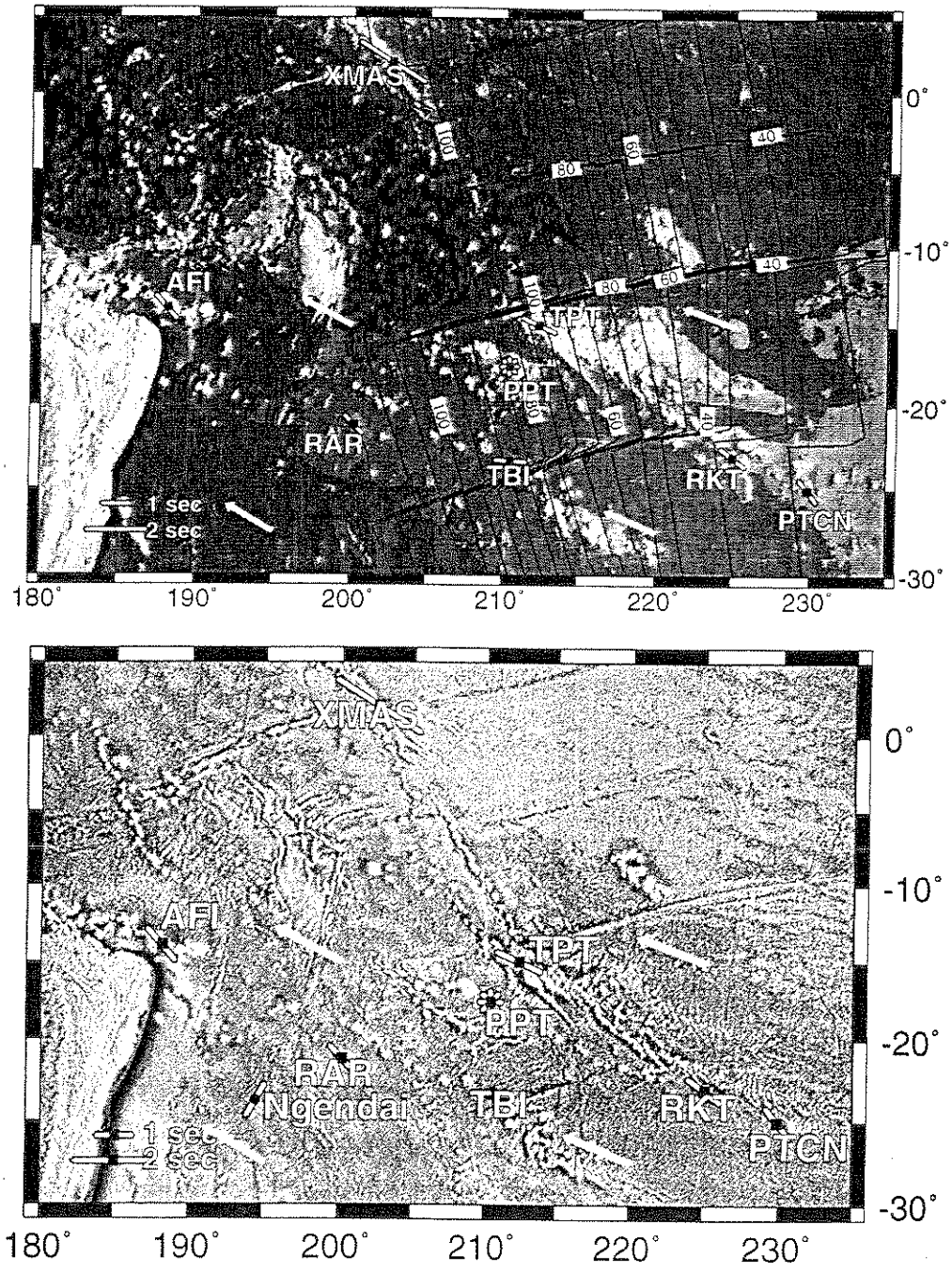


**Figure 6.** (a) Splitting parameters determined from stacks at TPT, PPT, and TBI stations shown; $\phi$ direction is parallel to bar shown at the two stations, TPT and TBI. Delay time is proportional to length of bar according to key, lower left. Azimuthal isotropy at PPT indicated by star. APM directions [*Gripp and Gordon*, 1990] shown as white arrows. Pacific lithosphere age [*Mueller et al.*, 1993] shown as thin black lines, ages as labeled. Splitting parameters at RAR and AFI from *Wolfe and Silver* [1998]. Note, except for PPT, $\phi$ directions in the south-central Pacific are nearly parallel to the APM direction. (b) Same as Figure 6a, but background is free-air gravity of *Sandwell and Smith* [1997]. Marquesas and Austral Fracture Zones (near stations TPT and TBI, respectively) are more clearly evident in the gravity field than in ETOP05.

then have to refreeze in the current APM direction. Lithospheric fabric reorientation would have to be a local phenomenon given the results of surface wave studies indicating little anisotropy in much of the western Pacific lithosphere. If the source of TPT splitting is reoriented lithospheric fabrics, then, given the motion history of the Pacific plate relative to Pacific hotspots, this lithospheric fabric must have developed after the change to current Pacific APM at 43 Ma [*Dalrymple and Clague*, 1976]. In this case, the major effects of Tu-

amotu Plateau formation on the local lithosphere would have had to take place after 43 Ma, unless such lithospheric recrystallization is pervasive and widespread.

### 7.2. PPT, Tahiti, Society Islands

Splitting parameters, and hence upper mantle seismic anisotropy, are highly variable between islands in French Polynesia, as exhibited by the different results at PPT and TPT, a mere 350 km apart. Splitting is clearly detected at TPT, but PPT is apparently underlain by an effectively azimuthally isotropic mantle. Given the small number of stations for which data exist, we can only speculate as to the meaning of this result: perhaps the absence of detectable upper mantle deformation at PPT is related to the recent (1 Ma) volcanism on the island. We note that if the symmetry axis of the anisotropic medium beneath PPT were vertical rather than horizontal, as we might expect if this volcanism were the result of the rise of magma within a hotspot conduit, we would detect no splitting. We infer that the different nature of the sites is of fundamental importance in this result: Tahiti is a young volcanic island ($\sim$ 1 Ma) with a typical "Hawaiian" crust [*Becker et al.*, 1974; *Calmant and Cazenave*, 1985] only 70 km away from an active underwater volcano, whereas Rangiroa (TPT) is an atoll sitting on the massive, 30 km thick crust of the Tuamotu Plateau [*Talandier and Okal*, 1987; *Ito et al.*, 1995]. This raises the question of the possible influence of young volcanism on shear wave splitting and on the local mantle flow pattern. More generally, the apparent variability of mantle deformation that we infer is at the root of this observation is most likely ascribable to the effects of hotspots on the lithosphere and asthenosphere at these island sites. With the exception of the Hawaiian chain, variability of island chain structure, geochemistry, and geochronology, and discrepancies between predictions concerning these parameters based on the hotspot model [*Morgan*, 1972] and their observations are the hallmark of the Pacific hotspot islands [*Okal and Batiza*, 1987].

### 7.3. TBI, Tubuai, Cook-Austral Chain

At TBI, on Tubuai in the Cook-Austral chain, the fast polarization direction is N86°W, 22° westward of the local Pacific APM direction (Figure 6) [*Gripp and Gordon*, 1990]. The trend of the nearby (70 km) Austral Fracture Zone is 25° southwestward of the TBI $\phi$ direction. Thus neither the asthenospheric (APM) nor fossil spreading (Austral Fracture Zone) hypothesis appears to explain uniquely the $\phi$ trend at TBI. We note that although the $\phi$ direction from the individual splitting measurement for TBI from the event on January 6, 1990 (N69°W; Table 1) is very close to the APM direction, the data for this event are nearly equally well fit by the splitting parameters derived from the multiple data procedure. Given the proximity of the station to the Austral Fracture Zone to TBI, the TBI $\phi$ direction, which lies between the APM and expected fossil direction, may indicate that the fracture zone structure perturbs asthenospheric flow beneath. However, comparison of their relative positions (Figure 6a) reveals that to the north, station TPT is almost equally close to the Marquesas Fracture Zone, without the attendant presumed perturbation. This difference could result from the greater thickness of crust [*Talandier and Okal*, 1987; *Ito et al.*, 1995] beneath the Tuamotu Plateau, relative to that of Tubuai and the Austral chain [*Calmant and Cazenave*, 1985].

### 7.4. RKT and PTCN, Pitcairn Chain

Splitting fast polarization trends about 15° northward of the local APM direction at station RKT. The uncertainty in the $\phi$ measurement ($\pm 6°$) reduces the possible angle between the fast-axis trend and APM to about 10°, and therefore the simplest interpretation of this measurement is that $\phi$ is close to the local APM. Thus similar arguments to those we outlined above for TPT can be invoked for this station: the anisotropic source is either the asthenospheric decoupling zone between the Pacific plate and underlying mesosphere with no contribution from fossil lithospheric spreading fabrics, or those lithospheric fabrics have somehow been erased and reoriented to nearly parallel the local APM direction.

Like the measurement at TBI, the preliminary $\phi$ direction we find for PTCN parallels neither the local APM trend nor the trends of nearby fracture zones. Note that Pitcairn Island is underlain by lithosphere some 23 m.y. old, formed well after the reorganization of the Pacific-Farallon Ridge, which occurred beginning around 30 Ma. Thus, fracture zones and APM are nearly parallel in this region, and the two possible choices for anisotropy source discussed throughout this paper are in fact reduced to an indistinguishable case: expected $\phi$ from APM and fossil spreading are parallel. We note that our measurement at Pitcairn is preliminary; however, $\phi$ at PTCN trends some 30° clockwise of the local APM and fossil spreading direction (NNW rather than WNW). The nearest major fracture zone is the Austral, which passes some 250 km north of Pitcairn Island trending WNW. This eastern extension of the Austral Fracture Zone is clearly visible in the recent 2-minute free-air gravity map of *Sandwell and Smith* [1997], corroborating the analysis of that fracture zone's morphology by *Okal and Cazenave* [1985]. If the measurement $\phi$ is assumed to be correct, then some process unrelated to either motion between lithosphere and mesosphere or formation of lithospheric spreading fabrics must have occurred to account for the splitting fast axis. The obvious candidate processes for PTCN are hotspot related mantle flow and/or lithospheric melting. The exact manner in which these processes might yield a fast polarization trend of N38°W is not obvious, however. Nonetheless, it seems likely that fabrics post-

dating original lithosphere formation cause the splitting, given the clear difference between the observed $\phi$ and expected and clearly defined fossil fabric orientation.

### 7.5. Comparison to Other South Pacific Island Stations

Although the indication of isotropy at PPT is unique so far in the Pacific basin, the measurements at TBI, TPT, RKT, and PTCN are similar to those made by *Wolfe and Silver* [1998] at AFI (Samoa) and RAR (Rarotonga) further west in the Cook-Austral chain. Both stations have $\phi$ directions that approximately parallel the local Pacific APM direction. Delay times at these stations are around 1 s, indicating an anisotropic layer approximately 100 to 120 km thick in the upper mantle beneath these stations. A preliminary examination of splitting at Kiritimati Island station XMAS by us yielded one split $S$ phase with $\phi$ of N58°W, and delay time of 2.5 s (Table 1), but the station has only been operating for a short time and no other data are yet available to confirm this result. However, in general, the results of available splitting analyses indicate that upper mantle deformation in the South Pacific is largely controlled by the current motion of the Pacific plate relative to the deeper mantle, as revealed by Pacific-hotspot relative motion. This result is consistent with results of regional (e.g., French Polynesia [*Okal and Talandier*, 1980]) and larger-scale [*Nishimura and Forsyth*, 1988, 1989; *Montagner and Tanimoto*, 1990, 1991] surface wave studies, and local $P_n$ azimuthal anisotropy studies [*Talandier and Bouchon*, 1979] that show that upper mantle anisotropy beneath this portion of the Pacific plate is parallel to the current local APM direction.

On the other hand, *Shearer and Orcutt* [1986] demonstrated the presence of both crustal and upper mantle anisotropy unrelated to Pacific APM at their Ngendai experiment site WSW of our study region. They attributed the mantle anisotropy to fossil fabrics formed at the original spreading ridge. However, as those authors note, magnetic anomalies that would clearly indicate trends of fracture zones (and thus of expected fossil lithospheric anisotropy) are absent from the area of the experiment (Figure 6). The mantle fast axis they obtained is N30°E, which lies at a high angle to all the measurements we present here, and to the nearest clearly defined fracture zones, which trend ENE. It seems clear that the fast direction they found is not related to current Pacific asthenosphere or it would have an APM fast axis; it is likely that this anisotropy is related to fossil lithosphere fabrics formed at a spreading ridge with significantly different trend from that of the younger seafloor we have studied.

## 8. Conclusions

The goals of our study were to determine shear wave splitting parameters at four islands in French Polynesia and on Pitcairn, to compare the resulting splitting fast-polarization directions ($\phi$) and delay times between fast and slow waves ($\delta t$) with local fossil spreading directions and Pacific motion directions relative to the hotspots, and to examine the relationship(s) between deformation of upper mantle lithosphere and/or asthenosphere, hotspot-related contributions to upper mantle deformation, and the coupling of the Pacific plate to its underlying mesosphere. Our analysis of shear wave splitting at island stations in French Polynesia reveals substantial differences in upper mantle deformation between the five stations we analyzed for shear wave splitting: TPT, on Rangiroa at the northwest end of the Tuamotu Plateau, has an APM-parallel $\phi$ direction and a delay time of 1.3 s; at PPT, on Tahiti, we could detect no splitting; and at TBI, on Tubuai in the Cook-Austral chain, we detected splitting with a delay time around 1 s, and a $\phi$ direction midway between the local APM direction and the fossil spreading direction, as locally indicated by the nearby Austral Fracture Zone. In the Pitcairn chain, we find splitting on Mangareva in the Gambiers (RKT) is close to APM-parallel, with a delay time of 1.1 s. On Pitcairn Island itself, the $\phi$ trend, N38°W, is not parallel to either local APM or expected lithospheric fossil spreading fabrics. Delay time at Pitcairn is 1.1 s, identical to those at TPT, TBI, and RKT. The simplest explanation of the variability of splitting parameters we find is that the upper mantle has deformed differently beneath the five sites. We interpret the measurements at TPT and RKT as indicating asthenospheric flow in the APM direction beneath the station. At PPT, apparent isotropy could indicate the presence of deformed upper mantle with a vertical symmetry axis or the absence of any strong and consistent mantle deformation fabric beneath Tahiti. Both effects could be related to recent hotspot magmatism on Tahiti. Isotropy could result from destruction of linear mantle fabrics by reheating and recrystallization of lithospheric olivine. Vertical symmetry axes could be a product of diapiric rise of magma and associated lithospheric deformation related to hotspot activity. At TBI, such asthenospheric flow may be complicated by the effect of juxtaposition of different lithospheric thicknesses along the nearby Austral Fracture Zone, resulting in perturbation of asthenospheric flow. The general absence of fossil spreading related splitting at all five sites indicates that mantle processes postdating lithosphere formation are important in the South Pacific.

**Acknowledgments.** We thank C. Wolfe and P. Silver for generously providing their joint splitting analysis code, and with their results, prepublication. We thank F. Schindelé and D. Reymond in Papeete for their invaluable help in extracting the data we used. The IRIS DMC provided data we used, for which we are very grateful. Many thanks to D. Sandwell and W. Smith for the use of their global marine free-air gravity data set. C. Bina, F. Boudier, P. Lundgren, J. Morgan, A. Nicolas, J. Phipps Morgan, T. Shoberg, P. Silver, N. Sleep, A. Tommasi, C. Wolfe, and M. Woods helped

us by freely discussing many aspects of this work and their related work. Many thanks also to Peter Shearer, Jim Gaherty, and Martha Savage for their helpful reviews of this paper. We used GMT by *Wessel and Smith* [1991, 1995] to make figures in this paper. This work was supported by CEA (France), NSF grants EAR 93-16457 to P. Silver and R. Russo, and EAR 91-05954 to E. A. Okal, and by an NSF-NATO Fellowship to R. Russo.

## References

Ansel, V., and H.-C. Nataf, Anisotropy beneath 9 stations of the Geoscope broadband network as deduced from shear-wave splitting, *Geophys. Res. Lett., 16*, 409-412, 1989.

Avé Lallemant, H. G., and N. L. Carter, Syntectonic recrystallization of olivine and modes of flow in the upper mantle, *Geol. Soc. Am. Bull., 81*, 2203-2220, 1970.

Babužska, V., J. Plomerova, and J. Šilený, Models of seismic anisotropy in the deep continental lithosphere, *Phys. Earth Planet. Inter., 78*, 167-191, 1993.

Becker, M., R. Brousse, G. Guille, and H. Bellon, Phases d'érosion-comblement de la vallée de la Papenoo et volcanisme sub-récent à Tahiti, en relation avec l'évolution des Iles de la Société, *Marine Geology, 16*, M71-M77, 1974.

Binard, N., R. Hékinian, and P. Stoffers, Morphostructural study and type of volcanism of submarine volcanoes over the Pitcairn hot spot in the South Pacific, *Tectonophysics, 206*, 245-264, 1992.

Bormann, P., G. Grünthal, R. Kind, and H. Montag, Upper mantle anisotropy underneath Central Europe: Effect of absolute plate motion and lithosphere-asthenosphere boundary topography?, *J. Geodyn., 22*, 11-32, 1996.

Bowman, J. R., and M. Ando, Shear-wave splitting in the upper-mantle wedge above the Tonga subduction zone, *Geophys. J. R. Astron. Soc., 88*, 25-41, 1987.

Calmant, S., and A. Cazenave, The elastic lithosphere under the Cook-Austral and Society Islands, *Earth Planet. Sci. Lett., 77*, 187-202, 1985.

Cara, M., and J.-J. Lévêque, Anisotropy of the asthenosphere: The higher mode data or the Pacific revisited, *Geophys. Res. Lett., 15*, 205-208, 1988.

Carter, N., D. Baker, and R. George, Seismic anisotropy, flow and constitution of the upper mantle, in *Flow and Fracture of Rocks, Geophys. Monogr. Ser.*, vol 16, edited by H. C. Heard et al., pp. 167-190, AGU, Washington, D. C., 1972.

Cheminée, J.-L., R. Hékinian, J. Talandier, F. Albarède, C.W. Devey, J. Francheteau, and Y. Lancelot, Geology of an active hotspot: Tahiti-Mehetia region in the Southcentral Pacific, *Mar. Geophys. Res., 11*, 27-50, 1989.

Dalrymple, G. B., and D. A. Clague, Age of the Hawaiian-Emperor bend, *Earth Planet. Sci. Lett., 31*, 313-329, 1976.

Dalrymple, G. B., R. D. Jarrard, and D. A. Clague, K/Ar ages of some volcanic rocks from the Cook and Austral Islands, *Geol. Soc. Am. Bull., 86*, 1463-1467, 1975.

Detrick, R. S., and S. T. Crough, Island subsidence, hot spots, and lithospheric thinning, *J. Geophys. Res., 83*, 1236-1243, 1978.

Duncan, R. A., and I. McDougall, Linear volcanism in French Polynesia, *J. Volcanol. Geotherm. Res., 1*, 197-227, 1976.

Duncan, R. A., I. McDougall, R. M. Carter, and D. S. Coombs, Pitcairn island - another Pacific hot spot? *Nature, 251*, 679-682, 1974.

Dupuy, C., P. Vidal, R. C. Maury, and G. Guille, Basalts from Mururoa, Fangataufa and Gambier islands (French Polynesia): Geochemical dependence on the age of the lithosphere, *Earth Planet. Sci. Lett., 117*, 89-100, 1993.

Epp, D., Possible perturbations to hotspot traces and implications for the origin and structure of the Line Islands, *J. Geophys. Res., 89*, 11,273-11,286, 1984.

Forsyth, D. W., The early structural evolution and anisotropy of the oceanic upper-mantle, *Geophys. J. R. Astron. Soc., 43*, 103-162, 1975.

Forsyth, D. W., and S. Uyeda, On the relative importance of the driving forces of plate motions, *Geophys. J. R. Astron. Soc., 43*, 163-200, 1975.

Francis, T., Generation of seismic anisotropy in the upper mantle along the mid-oceanic ridges, *Nature, 221*, 162-165, 1969.

Gaherty, J. B., and T. H. Jordan, Seismic structure of the upper mantle in a central Pacific corridor, *J. Geophys. Res., 101*, 22,291-22,309, 1996.

Gledhill, K., and D. Gubbins, SKS splitting and the seismic anisotropy of the mantle beneath the Hikurangi subduction zone, New Zealand, *Phys. Earth Planet. Inter., 95*, 227-236, 1996.

Gripp, A. E., and R. G. Gordon, Current plate velocities relative to the hotspots incorporating the NUVEL-1 global plate motion model, *Geophys. Res. Lett., 17*, 1109-1112, 1990.

Guéguen, Y., and A. Nicolas, Deformation of mantle rocks, *Annu. Rev. Earth Planet. Sci., 8*, 119-144, 1980.

Guillope, M., and J. P. Poirier, Dynamic recrystallization during creep of single-crystal halite: An experimental study, *J. Geophys. Res., 84*, 5557-5567, 1979.

Guillou, H., P.-Y. Gillot, and G. Guille, Age (K-Ar) et position des îles Gambier dans l'alignement du point chaud de Pitcairn (Pacifique Sud), *C. R. Acad. Sci., Ser. II, 318*, 635-641, 1994.

Gutenberg, B., Untersuchungen zur Frage, bis zu welcher Tiefe die Erde kristallin ist, *Z. Geophys., 2*, 24-29, 1926.

Hart, S. R., A large-scale isotope anomaly in the southern hemisphere mantle, *Nature, 309*, 753-757, 1984.

Helffrich, G. R., P. G. Silver, and H. K. Given, Shear wave splitting variation over short spatial scales on continents, *Geophys. J. Int., 119*, 561-573, 1994.

Hess, H. H., Seismic anisotropy of the uppermost mantle under oceans, *Nature, 203*, 629-631, 1964.

Ito, G., M. McNutt, and R. L. Gibson, Crustal structure of the Tuamotu Plateau, 15° S, and implications for its origin, *J. Geophys. Res., 100*, 8097-8114, 1995.

Jarrard, R. D., and D. A. Clague, Implications of Pacific island and seamount ages for the origin of volcanic chains, *Rev. Geophys. Space Phys., 15*, 57-75, 1977.

Kaneshima, S., and P. G. Silver, A search for source side mantle anisotropy, *Geophys. Res. Lett., 19*, 1049-1052, 1992.

Kennett, B. L. N., and E. R. Engdahl, Travel times for global earthquake location and phase identification, *Geophys. J. Int., 105*, 429-465, 1991.

Kuo, B.-Y., and D. W. Forsyth, A search for split *SKS* waveforms in the North Atlantic, *Geophys. J. Int., 108*, 557-574, 1992.

Mainprice, D. and P. G. Silver, Constraints on the interpretation of teleseismic *SKS* observations from kimberlite nodules from the subcontinental mantle, *Phys. Earth Planet. Inter., 78*, 257-280, 1993.

Montagner, J.-P., and H.-C. Nataf, A simple method for inverting the azimuthal anisotropy of surface waves, *J. Geophys. Res., 91*, 511-520, 1986.

Montagner, J.-P., and T. Tanimoto, Global anisotropy in the upper mantle inferred from the regionalization of phase velocities, *J. Geophys. Res., 95*, 4797-4819, 1990.

Montagner, J.-P., and T. Tanimoto, Global upper mantle tomography of seismic velocities and anisotropies, *J. Geophys. Res., 96*, 20,337-20,351, 1991.

Morgan, W. J., Plate motions and deep mantle convection, *Mem. Geol. Soc. Am., 132*, 7-22, 1972.

Morris, G. B., R. W. Raitt, and G. G. Shor Jr., Velocity anisotropy and delay-time maps of the mantle near Hawaii, *J. Geophys. Res., 74*, 4300-4316, 1969.

Mottay, G., Contribution à l'étude géologique de la Polynésie Française: Archipel des Australes Mehetia (Archipel de la Société), Thèse de 3ème cycle, Univ. Paris-Sud Orsay, 1976.

Mueller, R. D., W. R. Roest, J.-Y. Royer, L. M. Gahagan, and J. G. Sclater, A digital age map of the ocean floor, *Scripps Inst. of Oceanogr. Ref. Ser. 93-30*, Scripps Inst. of Oceanogr., La Jolla, Calif., 1993.

Nicolas, A., Structure and petrology of peridotites: Clues to their geodynamic environment, *Rev. Geophys., 24*, 875-895, 1986.

Nicolas, A., and N. I. Christensen, Formation of anisotropy in upper mantle peridotites: A review, in *Composition, Structure and Dynamics of the Lithosphere-Asthenosphere System, Geodynam. Ser.*, vol. 16, edited by K. Fuchs and C. Froidevaux, pp. 111-123, AGU, Washington, D. C., 1987.

Nishimura, C., and D. W. Forsyth, Rayleigh wave phase velocities in the Pacific with implications for azimuthal anisotropy and lateral heterogeneities, *Geophys. J. Int., 94*, 479-501, 1988.

Nishimura, C., and D. W. Forsyth, The anisotropic structure of the upper mantle in the Pacific, *Geophys. J. Int., 96*, 203-229, 1989.

Okal, E. A., and R. Batiza, Hotspots: The first 25 years, in *Seamounts, Islands and Atolls, Geophys. Monogr. Ser.*, vol. 43, edited by B. Keating et al., pp. 1-11, AGU, Washington, D. C., 1987.

Okal, E. A., and A. Cazenave, A model for the plate tectonic evolution of the east-central Pacific based on SEASAT investigations, *Earth Planet. Sci. Lett., 72*, 99-116, 1985.

Okal, E. A., and J. Talandier, Rayleigh wave dispersion in French Polynesia, *Geophys. J. R. Astron. Soc., 63*, 719-733, 1980.

Ribe, N. M., Seismic anisotropy and mantle flow, *J. Geophys. Res., 94*, 4213-4223, 1989.

Ribe, N. M., and Y. Yu, A theory for plastic deformation and textural evolution of olivine polycrystals, *J. Geophys. Res., 96*, 8325-8335, 1991.

Russo, R. M., and P. G. Silver, Trench-parallel flow beneath the Nazca plate from seismic anisotropy, *Science, 263*, 1105-1111, 1994.

Russo, R. M., P. G. Silver, M. Franke, W. B. Ambeh, and D. E. James, Shear wave splitting in northeast Venezuela, Trinidad, and the eastern Caribbean, *Phys. Earth Planet. Inter., 95*, 251-275, 1996.

Sandwell, D. T., and W. H. F. Smith, Marine gravity anomaly from Geosat and ERS-1 satellite altimetry, *J. Geophys. Res., 102*, 10,039-10,054, 1997.

Schlanger, S. O., M. O. Garcia, B. H. Keating, J. J. Naughton, W. W. Sager, J. A. Haggerty, J. A. Philpotts, and R. A. Duncan, Geology and geochronology of the Line Islands, *J. Geophys. Res., 89*, 653-678, 1984.

Shearer, P. M., and J. A. Orcutt, Compressional and shear-wave anisotropy in the oceanic lithosphere: the Ngendai seismic refraction experiment, *Geophys. J. R. Astron. Soc., 87*, 967-1003, 1986.

Silver, P. G., Seismic anisotropy beneath the continents: Probing the depths of geology, *Annu. Rev. Earth Planet. Sci., 24*, 385-432, 1996.

Silver, P. G., and W. W. Chan, Shear wave splitting and subcontinental mantle deformation, *J. Geophys. Res., 96*, 16,429-16,454, 1991.

Silver, P. G., and M. K. Savage, The interpretation of shear-wave splitting parameters in the presence of two anisotropic layers, *Geophys. J. Int., 119*, 949-963, 1994.

Sleep, N. H., Lithospheric thinning by midplate mantle plumes and the thermal history of hot plume material ponded at sublithospheric depths, *J. Geophys. Res., 99*, 9327-9343, 1994.

Stoffers, P., et al., Active Pitcairn hotspot found, *Mar. Geol., 95*, 51-55, 1990.

Su, L., and J. Park, Anisotropy and the splitting of *PS* waves, *Phys. Earth Planet. Inter., 86*, 263-276, 1994.

Talandier, J., and M. Bouchon, Propagation of high-frequency $P_n$ waves at great distances in the South Pacific and its implication for the structure of the lower lithosphere, *J. Geophys. Res., 84*, 5613-5619, 1979.

Talandier, J., and G. T. Kuster, Seismicity and submarine volcanic activity in French Polynesia, *J. Geophys. Res., 81*, 936-948, 1976.

Talandier, J., and E. A. Okal, The volcanoseismic swarms of 1981-1983 in the Tahiti-Mehetia area, French Polynesia, *J. Geophys. Res., 89*, 11,216-11,234, 1984.

Talandier, J., and E. A. Okal, Crustal structure in the Tuamotu and Society Islands, French Polynesia, *Geophys. J. R. Astron. Soc., 88*, 499-528, 1987.

Tanimoto, T., and D. L. Anderson, Lateral heterogeneity and azimuthal anisotropy of the upper mantle: Love and Rayleigh waves 100-250 s, *J. Geophys. Res., 90*, 1842-1858, 1985.

Tommasi, A., A. Vauchez, and R. Russo, Seismic anisotropy in oceanic basins: Resistive drag of the sublithospheric mantle?, *Geophys. Res. Lett., 23*, 2991-2994, 1996.

Turner, D. L., and R. D. Jarrard, K/Ar dating of the Cook-Austral Island chain: A test of the hot spot hypothesis, *J. Volcanol. Geotherm. Res., 12*, 187-220, 1982.

Vinnik, L. P., and R. Kind, Ellipticity of teleseismic *S*-particle motion, *Geophys. J. Int., 113*, 165-174, 1993.

Vinnik, L. P., V. Farra, and B. A. Romanowicz, Azimuthal anisotropy in the Earth from observations of *SKS* at Geoscope and NARS broadband stations, *Bull. Seismol. Soc. Am., 79*, 1542-1558, 1989.

Vogt, P. R., and G. L. Johnson, Transform faults and longitudinal flow below the midoceanic ridge, *J. Geophys. Res., 80*, 1399-1428, 1975.

Wessel, P., and W. H. F. Smith, Free software helps map and display data, *Eos Trans. AGU, 72*, pp. 441,445-446, 1991.

Wessel, P., and W. H. F. Smith, New version of the Generic Mapping Tools released, *Eos Trans. AGU, 76*, 329, 1995.

Wolfe, C. J., and P. G. Silver, Seismic anisotropy of oceanic upper mantle: Shear wave splitting methodologies and observations, *J. Geophys. Res., 103*, 749-771, 1998.

Woodhead, J. D., and M. T. McCulloch, Ancient seafloor signals in Pitcairn Island lavas and evidence for large amplitude, small length-scale mantle heterogeneities, *Earth Planet. Sci. Lett., 94*, 257-273, 1989.

Yang, X., K. M. Fischer, and G. A. Abers, Seismic anisotropy beneath the Shumagin Islands segment of the Aleutian-Alaska subduction zone, *J. Geophys. Res., 100*, 18,165-18,177, 1995.

E. A. Okal and R. M. Russo, Department of Geological Sciences, Northwestern University, Evanston, IL 60208. (email: ray@earth.nwu.edu)

(Received July 7, 1997; revised February 26, 1998; accepted March 19, 1998.)